PNAS
www.pnas.org

Supplementary Information for

Physical tuning of galectin-3 signaling

Shaheen A. Farhadi[a], Renjie Liu[a], Matthew W. Becker[a], Edward A. Phelps[a], and Gregory A. Hudalla[a,1]

[a]J. Crayton Pruitt Family Department of Biomedical Engineering, University of Florida, Gainesville, FL, 32611, USA

[1]Corresponding author:
Gregory A. Hudalla, PhD
Email: ghudalla@bme.ufl.edu

This PDF file includes:

Supplementary text
Table S1
Figures S1 to S20

Other supplementary materials for this manuscript include the following:

Notes S1 to S2

Supplementary Information Text

Materials and Methods

Cloning, expression, and purification of proteins. Genes encoding protein constructs were inserted into pET-21d(+) vectors between NcoI and XhoI restriction sites. All genetic and amino acid sequences are provided in the *SI Appendix*, Notes S1 and S2, respectively. GenBank accession codes are also provided for Monomer (MH92054), Dimer (MW252053), Trimer (MH92055), Tetramer (MW252054), Pentamer (MW252055), and Hexamer (MW252056). Plasmids were transformed into Origami™ B (DE3) *E. coli* (Novagen®) and selected on ampicillin (100 µg/mL) and kanamycin B (15 µg/mL) doped LB/agar plates overnight at 37 °C. A single colony was selected and inoculated in 5 ml of lysogeny broth (LB) containing ampicillin (100 µg/mL) and kanamycin B (15 µg/mL). Cultures were grown overnight at 37 °C, 225 rpm on an orbital shaker before being sub-cultured into 1 L 2xTY media (16 g tryptone, 10 g yeast extract, 5 g NaCl) containing ampicillin (100 µg/mL) and kanamycin B (15 µg/mL). Cultures continued to grow at 37 °C, 225 rpm until reaching an optical density of 0.6-0.8 at wavelength, λ = 600 nm. Cultures were then supplemented with 0.5 mM isopropyl β-D-1-thiogalactopyranoside (IPTG) (ThermoFisher) to induce protein expression and incubated for 18 h at 18 °C, 225 rpm. Bacteria were pelleted and washed with phosphate buffered saline (1x PBS, pH 7.4) via centrifugation (11,300 x *g* at 4 °C for 10 min) with a Sorvall™ RC 6 Plus Superspeed Centrifuge (ThermoFisher). Bacteria pellets were then mechanically disrupted with a spatula and lysed in B-PER bacterial protein extraction reagent (ThermoFisher) supplemented with a Pierce protease inhibitor tablet (ThermoFisher), 2,400 units/mL DNAse I (ThermoFisher), and 50 mg/mL lysozyme (ThermoFisher) for 20 min at room temperature. Bacterial lysate was further resuspended in immobilized metal affinity chromatography (IMAC) wash buffer (1x PBS with 20 mM imidazole). The bacterial lysate was then centrifuged (42,600 x *g* at 4 °C for 15 min) to separate the soluble protein fraction, which was collected from the supernatant. Proteins of interest were purified from the soluble protein fraction via IMAC. Briefly, His-tagged proteins of interest from the soluble fraction were loaded onto HisTrap™ FF Crude Prepacked Columns (GE Healthcare) connected to an ÄKTA™ pure FPLC system (GE Healthcare). In general, a gradient of 0-250 mM imidazole was used to elute proteins of interest bound to the columns. However, protein constructs containing multiple 6xHis-tags were collected from columns over a broader elution profile using a gradient of 0-500 mM imidazole. Amicon® Ultra Centrifugal Filters (MilliporeSigma) with 10 kDa or 50 kDa cut-off were used to concentrate IMAC-purified proteins to 5 mL for further purification and removal of imidazole via size-exclusion chromatography (SEC). Eluted protein fractions corresponding with major absorbance peaks were collected from a HiLoad™ 26/600 Superdex™ 200 pg column (GE Healthcare) connected to an ÄKTA™ pure FPLC system. Purity of proteins collected from SEC was analyzed using sodium dodecyl sulfate polyacrylamide gel electrophoresis (SDS-PAGE) and Coomassie staining. Endotoxin content from purified proteins was reduced below 1.0 EU/mL, using Pierce™ High Capacity Endotoxin Removal Spin Columns (ThermoFisher). Final endotoxin content was determined with a Pierce LAL Chromogenic Endotoxin Quantitation Kit (ThermoFisher), according to the manufacturer's instructions. Molar concentration of proteins was determined by Beer-Lambert Law. Absorbance (λ = 280 nm) was measured on a NanoDrop spectrophotometer (ThermoFisher) and extinction coefficient of each protein was calculated based on amino acid content using ExPASy ProtParam tool (available at https://web.expasy.org/protparam/). Extinction coefficients are as follows: 2052.5 $M^{-1}mm^{-1}$ for sfGFP; 3587 $M^{-1}mm^{-1}$ for Gal3; 5639.5 $M^{-1}mm^{-1}$ for Monomer; 5788.5 $M^{-1}mm^{-1}$ for Dimer, Trimer, and Tetramer; 6189.5 $M^{-1}mm^{-1}$ for Pentamer and Hexamer. A free software for biomolecular illustration (53) was used to illustrate sfGFP and Gal3 CRD shown in schematics.

Protein size analysis. Denatured protein molecular weight was determined based on their electrophoretic mobilities under denaturing conditions alongside a protein ladder (BP3602500, ThermoFisher) (*SI Appendix*, Fig. S2 *B* and *C*). Native protein size was determined via SEC. Briefly, proteins were prepared in 1x PBS (250 µL, 15 µM) and loaded onto a Superdex™ 200 10/30 GL column (GE Healthcare) connected to an ÄKTA™ pure FPLC system. Proteins that eluted from the column were detected at wavelength, λ = 280 nm and the data were normalized based on maximum signal intensity. Native protein molecular weight was calculated from a SEC calibration curve

prepared from protein standard markers (Bio-Rad, GE Healthcare, ThermoFisher). Next, protein hydrodynamic size was characterized by dynamic light scattering (DLS). Prior to taking these DLS measurements, proteins were prepared in 1x PBS (250 µL, 15 µM), filtered through a 0.2-micron syringe filter, and equilibrated to room temperature. Molar concentration of proteins was measured before and after filtration to ensure no significant amount of protein was lost due to aggregation. DLS measurements were taken on a NanoBrook 90Plus Particle Size Analyzer and BIC Particle Sizing Software (Brookhaven Instruments) in technical triplicate after ten 30 s runs. Hydrodynamic diameter ± standard deviation normalized by number-weighted size distribution were collected from the DLS instrument.

Reporter protein activity assays. In all reporter protein activity assays, molar concentration of protein constructs was adjusted on a per mole of sfGFP basis using a NanoDrop spectrophotometer at λ = 280 nm. Standard curves of sfGFP molar concentration versus relative fluorescence units (RFU) were produced by serial dilution of proteins ([sfGFP] = 1-0 µM) in black, clear plastic bottom 96-well microplates (*SI Appendix*, Fig. S4*A*). RFU were measured using excitation/emission 485/510 nm with a cutoff of 495 nm on a SpectraMax® M3 Multi-Mode microplate reader (Molecular Devices). Additionally, fluorescence spectra were plotted between 485-600 nm in 1 nm increments at [sfGFP] = 1 µM using the same settings describe above (*SI Appendix*, Fig. S4*B*).

Carbohydrate and glycoprotein binding assays. In all binding assays, molar concentration of protein constructs was adjusted on a per mole of Gal3 basis. Lactose binding affinity was evaluated using lactose affinity chromatography on an ÄKTA pure FPLC system. Briefly, a Tricorn™ 5/50 column (GE Healthcare) was packed with α-lactose-agarose resin (L7634, MilliporeSigma) according to manufacturer instructions (GE Healthcare). A volume of 500 µl of protein construct ([Gal3] = 30 µM) was applied to the α-lactose-agarose column and then washed with 10 column volumes of 1x PBS to remove unbound protein. Subsequently, protein that remained bound to the α-lactose-agarose column was eluted with a linear gradient of 0-100 mM soluble β-lactose (AAH54447A1, ThermoFisher) in 1x PBS. Proteins that eluted from the column were detected at λ = 280 nm and the data were normalized based on maximum signal intensity.

Saturation binding of protein constructs to surface-adsorbed asialofetuin (ASF) were generated through previously established methods (28). Briefly, black, clear plastic bottom 96-well microplates were coated with 100 µL of 50 µg/mL ASF (A4781, MilliporeSigma) for 2 h at 37 °C. The supernatant was then removed, and wells were washed with 1x PBS followed by a 100 µL of 1% bovine serum albumin (ThermoFisher) blocking step for 1 h at room temperature. The supernatant was removed once more, and wells were washed with 1x PBS. Next, 100 µL of increasing molar concentration of protein constructs ([Gal3] = 0-10 µM) were incubated with ASF within wells for 1 h at room temperature. The supernatant was again removed, and wells were washed for a total of three times with 1x PBS. Finally, sfGFP fluorescence was detected from bound protein constructs via a SpectraMax® M3 Multi-Mode microplate reader. Molar concentration of bound sfGFP was calculated using a standard curve, as described above, and then data were fit through non-linear regression analysis on GraphPad Prism software.

Competitive binding inhibition curves were generated using previously established methods (28). Briefly, black, clear plastic bottom 96-well microplates were coated with ASF, blocked, and washed, as described above. Protein constructs were mixed with a range of 0-25 mM soluble LacNAc (A7791, MilliporeSigma) in 1x PBS at a 1:1 volume ratio (50 µL protein:50 µL LacNAc) where final [sfGFP/Gal3] = 0.5 µM, and then mixed solutions were added to adsorbed ASF for 1 h at room temperature. Unbound protein was removed, and wells were washed for a total of four times with 1x PBS. Bound sfGFP concentration was determined with a SpectraMax® M3 Multi-Mode microplate reader and standard curve, as described above. Bound signal was subtracted by a minimum signal (e.g., 10 mM LacNAc + protein) and divided by a maximum signal (e.g., 0 mM LacNAc + protein) to normalize the data. Normalized data were fit via non-linear regression analysis on GraphPad Prism software. Thereafter, half-maximal inhibitory concentration (IC50) was approximated from the normalized curve.

Cell binding assays. For all cell binding experiments, Jurkat (Clone E6-1, TIB-152™, ATCC®), J45.01 (CRL-1990™, ATCC®), and HuT 78 (TIB-161™, ATCC®) T cells were expanded in complete media (RPMI 1640 supplemented with 10% heat-inactivated fetal bovine serum, 1% penicillin–streptomycin, 200 mM L-glutamine, 1% HEPES buffer) at 37 °C, 5% CO_2. Note that the J45.01 T cell line derived from the Jurkat T cell line by first lysing cells in $CD45^+$ Jurkat T cell population and then clonally expanding the remaining CD45 deficient cells. The CD7 deficient HuT 78 T cell line was derived from a different patient source than the $CD7^+$ Jurkat T cell line. It is known that CD45 levels differ between Jurkat T cell line and HuT 78 T cell line. Nonetheless, all three cell lines are established models for characterizing Gal3 signaling (37). Expanded cells were aliquoted into 12 x 75 mm sterile, round bottom polystyrene test tubes, centrifuged (500 x *g* for 5 min at room temperature). Then, cells were resuspended to 200,000 cells/tube in serum-free media (i.e., complete media without 10% heat-inactivated fetal bovine serum) for fluorescence imaging or resuspended in complete media for flow cytometric binding analysis. In both experiments, protein constructs prepared in sterile 1x PBS were added to cells at an equal volume (100 µL protein + 100 µL cells) with molar concentration (final [Gal3] = 5 µM) adjusted on a per mole Gal3 basis. Protein constructs were incubated with cells for 30 min at 37 °C, 5% CO_2. Cells were then washed with 1 mL ice-cold 1x PBS with or without 100 mM soluble β-lactose, and then again with 1 mL ice-cold 1x PBS at 500 x *g* for 5 min 4 °C. Cells were resuspend to a final volume of 300 µL ice-cold 1x PBS and either transferred to an uncoated µ-Slide 8 Well glass bottom chamber coverslip (80821, ibidi®) for fluorescence imaging or placed on ice for subsequent flow cytometric analysis. Images of fluorescently labeled cells were acquired on a Zeiss Axio Observer inverted microscope with 40x/0.95 numerical aperture Korr M27 Plan-Apochromat objective and fluorescent filter set for green fluorescent protein (excitation λ = 480-490 nm and emission λ = 500-550 nm) at an exposure time set equal to 3 s. All images were taken under uniform acquisition settings and are displayed as such. Fluorescence signal, in terms of mean fluorescence intensity (MFI) of protein-bound cells was measured using a BD FACSCelesta™ flow cytometer equipped with BD FACSDiva™ software and a blue laser for FITC detection (excitation λ = 494 nm and emission λ = 519 nm, filters 530/30). Data were analyzed and graphed as histograms with FlowJo™ software or bar plots in GraphPad Prism software and percentage of difference between MFI of cells in conditions with and without added soluble β-lactose were calculated. Gating strategy for flow cytometric analysis of cell binding is provided in *SI Appendix*, Fig. S17.

Cell death assays. Cell death was determined via differential staining of BV421 Annexin V (563973, BD Biosciences) and LIVE/DEAD Near-IR dye (L34975, Invitrogen) and flow cytometric analysis. For all cell death assays, molar concentration of protein constructs was adjusted on a per mole of Gal3 basis. Jurkat, J45.01, and HuT 78 T cells were expanded in complete media, aliquoted at 200,000 cells/tube, and combined with protein constructs or wild-type Gal3 (final [Gal3] = 5 µM) prepared in sterile 1x PBS at an equal volume (100 µL protein + 100 µL cells). For positive single stain controls, cells were treated with either 250 ng/mL anti-Fas antibody (clone CH11, MilliporeSigma) or 1 µM (S)-(+)-camptothecin (C9911, MilliporeSigma). Cells were incubated for either 4 h or 18 h at 37 °C, 5% CO_2. After incubation, half the volume of cells treated with (S)-(+)-camptothecin was pipetted into a sterile microcentrifuge tube and heated to 56 °C for 5 min then cooled on ice for 5 min before returning to the other half of (S)-(+)-camptothecin-treated cells. Cells were washed with 100 mM soluble β-lactose in ice-cold 1x PBS and pelleted via centrifugation (500 x *g* for 5 min at 4 °C). Cells were then resuspended in 1 mL ice-cold, sterile 1x PBS, stained with 1 µL of stock LIVE/DEAD Near-IR dye, and kept on ice for 30 min while protected from light. Thereafter, cells were washed with ice-cold 1x PBS and pelleted via centrifugation (500 x *g* for 5 min at 4 °C). The supernatant was discarded and then cells were resuspended in 100 µL of 1x Annexin V Binding Buffer (556454, BD Biosciences) and 5 µL BV421 Annexin V. After gently mixing, cells were incubated for 15 min at room temperature while protected from light. An additional 200 µL of 1x Annexin V Binding Buffer was added to the cells before measurements were taken on BD FACSCelesta™ flow cytometer equipped with BD FACSDiva™ software. The following lasers were used for detection of BV421, sfGFP, and LIVE/DEAD Near-IR: violet/BV421 laser (excitation λ = 407 nm and emission λ = 421 nm, filters 450/40), blue/FITC laser (excitation λ = 494 nm and emission λ = 519 nm, filters 530/30), and red/APC-Cy™7 laser (excitation λ = 650 nm and emission λ = 785 nm, filters 780/60). Untreated control (i.e., PBS-treated cells) was used

alongside single stain controls for fluorescence compensation. Scatter plot quadrant data were acquired from FlowJo™ software and used to calculate percentage of cell death: [(% annexin V^- and LIVE/$DEAD^-$ cells in untreated group) − (% annexin V^- and LIVE/$DEAD^-$ cells in treated group)] / (% annexin V^- and LIVE/$DEAD^-$ cells in untreated group). Negative percentages were reported as zero percent.

Caspase-dependence of cell death signaling was determined using the pancaspase inhibitor Q-VD-OPh (563828, BD Biosciences). Jurkat, J45.01, and HuT 78 T cells were expanded and aliquoted into tubes, as described above. Next, cells were incubated in the presence or absence 1 µL of Q-VD-OPh (final [Q-VD-OPh] = 50 µM) or 1 µL vehicle control (final 0.5% DMSO) for 30 min at 37 °C, 5% CO_2. Cells were then combined with Hexamer or wild-type Gal3 (final [Gal3] = 5 µM) prepared in sterile 1x PBS at an equal volume (100 µL protein + 100 µL cells). Afterward, cells were washed, stained with BV421 Annexin V and LIVE/DEAD Near-IR dye, and analyzed using the same procedures described above. Gating strategy for flow cytometric analysis of cell death is provided in *SI Appendix*, Fig. S18.

Cell agglutination assays. Jurkat, J45.01, and HuT 78 T cells were expanded in complete media at 37 °C, 5% CO_2, as described above. Cells were aliquoted at 20,000 cells/well in sterile, clear, tissue culture-treated 96-well microplates. Protein constructs and wild-type Gal3 prepared in sterile 1x PBS were then added to cells at an equal volume (50 µL protein + 50 µL cells) with molar concentration (final [Gal3] = 5 µM) adjusted on a per mole Gal3 basis. Subsequently, cells were incubated for either 4 h or 18 h at 37 °C, 5% CO_2. Brightfield micrographs of cells were then taken with a Zeiss Axio Observer inverted microscope.

Membrane glycoprotein staining and confocal fluorescence microscopy. Protocols for immunofluorescence staining were adapted from Stillman and colleagues (37). Jurkat, J45.01, and HuT 78 T cells were expanded in complete media at 37 °C, 5% CO_2, as described above. Cells were aliquoted at 200,000 cells/tube and combined with either 1x PBS or Hexamer (final [Gal3] = 5 µM) prepared in sterile 1x PBS at an equal volume (100 µL protein + 100 µL cells). Cells were next incubated for 2 h at 37 °C, 5% CO_2. Afterward, cells were suspended in 1 mL 2% paraformaldehyde in 1x PBS on ice for 30 min. Fixation was quenched by adding 1 mL 400 mM glycine (final [glycine] = 200 mM) in 1x PBS for 5 min on ice. Subsequently, cells were pelleted via centrifugation (500 x *g* for 5 min at 4 °C) and then washed with ice-cold 1x PBS (500 x *g* for 5 min at 4 °C). Cells were next resuspended in 1 mL 10% goat serum blocking solution (50062Z, ThermoFisher) for 30 min at room temperature. Subsequently, 1 uL of monoclonal antibody from stock vial of mouse anti-human CD45 (Clone HI30, 555480, BD Biosciences), mouse anti-human CD7 (Clone M-T701, 555359, BD Biosciences), or mouse IgG1, κ isotype control (Clone MOPC-21, 555746, BD Biosciences) was added to cells (final [primary/isotype antibody] = 5 µg/mL) for 1 h on ice. Cells were pelleted via centrifugation (500 x *g* for 5 min at 4 °C) and then washed with ice-cold 1x PBS (500 x *g* for 5 min at 4 °C). Cells were next resuspended in 1 mL 10% goat serum blocking solution for 30 min at room temperature. Then, 1 uL of secondary antibody from stock vial of Alexa Fluor 568 goat anti-mouse IgG (A-11004, ThermoFisher) was added to cells (final [secondary antibody] = 2 µg/mL) for 1 h on ice. Next, cells were pelleted via centrifugation (500 x *g* for 5 min at 4 °C) and double washed with ice-cold 1x PBS (500 x *g* for 5 min at 4 °C). Cells were resuspended in approximately 100 µL 1x PBS, transferred to an uncoated µ-Slide 8 Well glass bottom chamber coverslip (80821, ibidi®), and mounted using 100 µL Prolong™ Glass Antifade Mountant (P36982, ThermoFisher) or ibidi® Mounting Medium (50001, ibidi®). Nonspecific staining and compensation between fluorescent channels were controlled using isotype-treated and single-stained cells (*SI Appendix*, Fig. S19). Confocal images (pinhole = 1 airy unit) of fluorescently labeled cells were acquired on a confocal laser-scanning microscope (Leica SP8) with 63x/1.40 numerical aperture Plan-Apochromat oil-immersion objective at 1,024 x 1,024-pixel resolution, 1.58 µs pixel dwell time, and 2 sequences between lines. Cells were scanned by sequential excitation of GFP (excitation λ = 488 nm and emission λ = 492-549 nm) and Alexa Fluor 568 (excitation λ = 552 nm and emission λ = 582-657 nm) fluorescent probes. Fluorescent images were acquired in separate channels at 7.229-µm optical slices. Images were converted into JPEG format using ImageJ and then brightness/contrast was adjusted uniformly for enhanced image quality of cropped

photos in Fig. 4 *B* and *C*. Unadjusted and uncropped images are shown in *SI Appendix*, Figs. S11 and S12.

Caspase activity measurements. For all caspase activity assays, Jurkat T cells were expanded in complete media, as described above. For analysis of caspase-8 activity, cells were aliquoted at 800,000 cells/well into a sterile, tissue culture-treated 48-well microplate. Hexamer and wild-type Gal3 prepared in sterile 1x PBS were then added to cells at an equal volume (100 µL protein + 100 µL cells) with molar concentration (final [Gal3] = 5 µM) adjusted on a per mole Gal3 basis. Cells incubated with proteins for 18 h at 37 °C, 5% CO_2. Afterward, cells were transferred to a sterile, V-bottom 96-well microplate and washed via centrifugation (500 x *g* for 5 min) on a centrifuge equipped with a microplate rotor. Pelleted cells were then processed according to manufacturer instructions of a commercially available caspase-8 activity assay kit (FLICE/Caspase-8 Colorimetric Assay Kit, K113100, ThermoFisher). Caspase-8 activity was detected at absorbance λ = 405 nm and data were reported as fold change relative to untreated control (PBS-treated cells).

For analysis of caspase-3/-7 activity, Jurkat T cells were aliquoted at 400,000 cells/well into a sterile, tissue culture-treated 96-well microplate. Hexamer and wild-type Gal3 prepared in sterile 1x PBS were then added to cells at an equal volume (50 µL protein + 50 µL cells) with molar concentration (final [Gal3] = 5 µM) adjusted on a per mole Gal3 basis. Afterward, cells were transferred to a sterile, V-bottom 96-well microplate and washed via centrifugation (500 x *g* for 5 min) on a centrifuge equipped with a microplate rotor. The supernatant was carefully pipetted from the wells without disrupting the cell pellet and stored frozen at -80 °C for later quantitation of secreted IL-2. Pelleted cells were then processed according to manufacturer instructions of a commercially available caspase-3/-7 activity assay kit (EnzCheck® Caspase-3 Assay Kit #1, E13183, ThermoFisher). Specifically, caspase-3/-7 activity was detected by proteolytic cleavage of aminomethylcoumarin (AMC)-derived substrate, Z-DEVD-AMC, with excitation/emission 342/441 nm.

Secreted IL-2 quantitation assay. For quantitation of secreted IL-2, Jurkat T cells were expanded in complete media, aliquoted, and treated with Hexamer and wild-type Gal3 using the same procedures in the caspase-3/-7 activity assay above. Frozen supernatants from the above caspase-3/-7 assay were thawed and evaluated for IL-2 content via manufacturer instructions of a commercially available solid-phase ELISA kit (Quantikine® Human IL-2 Immunoassay, D2050, R&D systems). Specifically, IL-2 levels were quantified based on substrate cleavage (absorbance λ = 450 nm) with an enzyme-linked polyclonal antibody specific for IL-2, and then data were converted into molar concentration based on a standard curve.

TO-PRO-3 uptake assay. Caspase-mediated pannexin-1 hemichannel opening was monitored by cellular uptake of TO-PRO-3 (T3605, Invitrogen), pannexin-1 inhibition with trovafloxacin (PZ0015, Sigma), and caspase inhibition with Q-VD-OPh, according to previously established methods (42). In this assay, concentration of Hexamer and wild-type Gal3 was adjusted on a per mole of Gal3 basis. Jurkat T cells were expanded, aliquoted, and incubated in the presence or absence of 1 µL Q-VD-OPh (final [Q-VD-OPh] = 50 µM).Then, cells were treated with Hexamer and wild-type Gal3 as described for the cell death assay protocols above. As positive control for pannexin-1 opening and selective TO-PRO-3 uptake, cells were treated with 250 ng/mL anti-Fas antibody for 4 h. Cells treated with Hexamer and wild-type Gal3 were incubated for 4 h, 8 h, 12 h, and 18 h. Afterward, cells were incubated with 1 µL of trovafloxacin (final [trovafloxacin] = 50 µM) for 20 min at 37 °C, 5% CO_2 and then 1 µL of TO-PRO-3 (final [TO-PRO-3] = 50 µM) for 10 min at room temperature while protected from light. Cells were finally washed with 1x PBS, stained with BV421 Annexin V, and analyzed using the same procedure described for the cell death assay protocols above. The following lasers were used for detection of BV421, sfGFP, and TO-PRO-3: violet/BV421 laser (excitation λ = 407 nm and emission λ = 421 nm, filters 450/40), blue/FITC laser (excitation λ = 494 nm and emission λ = 519 nm, filters 530/30), and red/APC laser (excitation λ = 660 nm and emission λ = 660 nm, filters 670/30). Gating strategy for flow cytometric analysis of TO-PRO-3 uptake is provided in *SI Appendix*, Fig. S20.

Statistical analysis. Experimental and control groups were $n \geq 3$ for DLS, reporter protein activity, ASF binding, cell binding, cell death, cell agglutination, caspase activity, IL-2 secretion, and TO-PRO-3 uptake studies. Statistical significance was reported by analyzing data sets using unpaired, two-tailed Student's t-test or one-way ANOVA with Tukey's multiple comparison test in GraphPad Prism software. Outliers in data were identified with Grubbs' test and removed. Mean and standard deviations were reported for all replicated studies and statistical differences were defined as significant at $p < 0.05$ or NS if not significant.

Protein	Denatured molecular weight (kDa)		Native molecular weight (kDa)		Hydrodynamic diameter (nm)
	Empirical	Predicted	Empirical	Predicted	Empirical
WT-Gal3	28.4	27.2	19.6	27.2	-
sfGFP	27.6	27.9	26.8	27.9	-
Monomer	55.2	55.1	52.9	55.1	5.2 ± 0.7
Dimer	59.8	60.4	137.3	120.7	9.3 ± 1.8
Trimer	59.8	60.3	181.5	180.9	10.3 ± 0.2
Tetramer	59.8	60.4	222.7	241.5	12.6 ± 0.1
Pentamer	59.8	59.7	290.5	298.6	13.1 ± 0.8
Hexamer	59.8	59.5	353.4	356.8	14.6 ± 1.7

Table S1. Physical properties of wild-type proteins and synthetic Gal3 constructs.

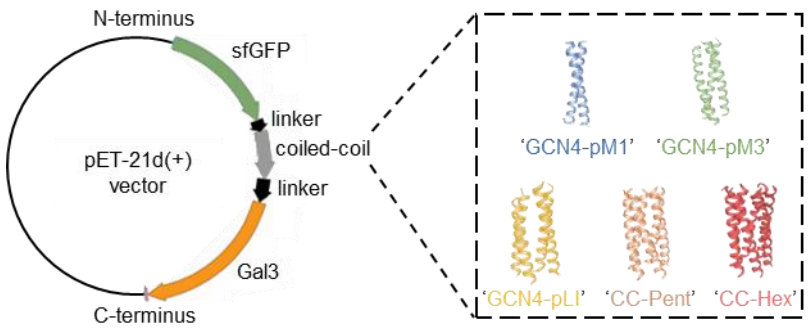

Fig. S1. Recombinant fusion strategy incorporating parallel, α-helical coiled-coil scaffolds for construction of synthetic Gal3 oligomers.

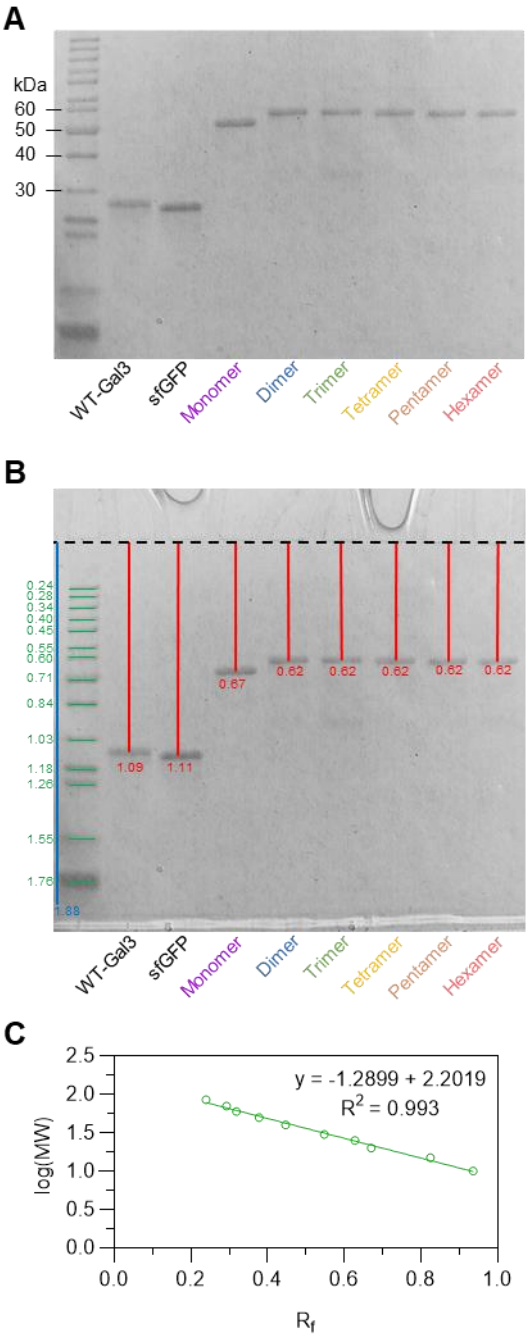

Fig. S2. SDS-PAGE gel of purified proteins. (*A*) PAGE gel without migration distances measured. (*B*) PAGE gel with migration distances measured (i.e., relative mobility, R_f). (*C*) Standard curve of log(molecular weight, MW) versus R_f for approximation of denatured molecular weight of proteins.

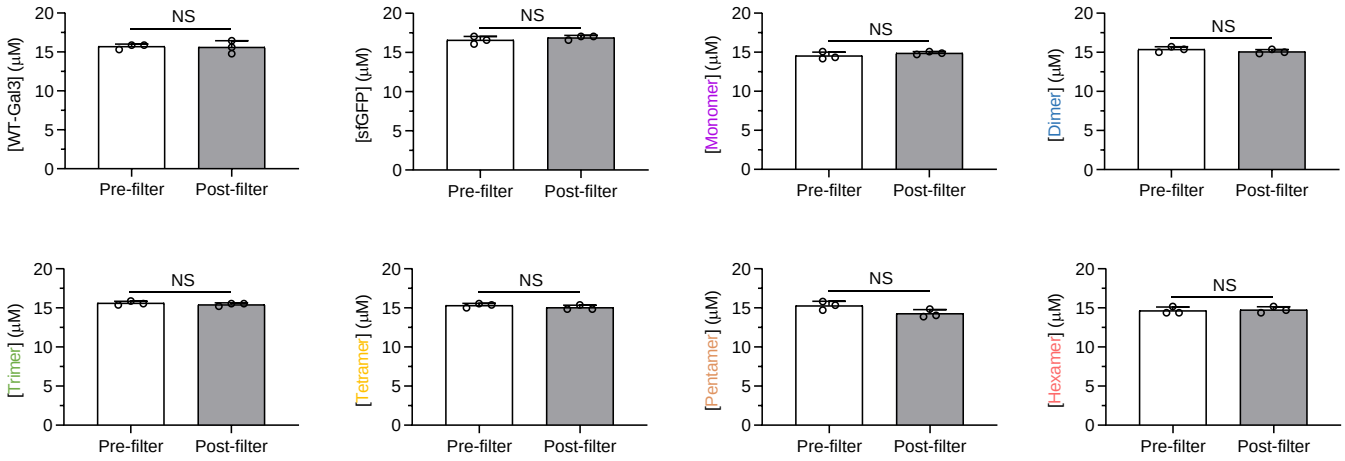

Fig. S3. Molar concentration of synthetic Gal3 constructs before (white bar) and after (gray bar) filtration with a 0.2-micron syringe filter for dynamic light scattering experiments. *n* = 3, mean ± s.d., NS is no significant difference, and statistical comparisons were made using unpaired two-tailed Student's t-test.

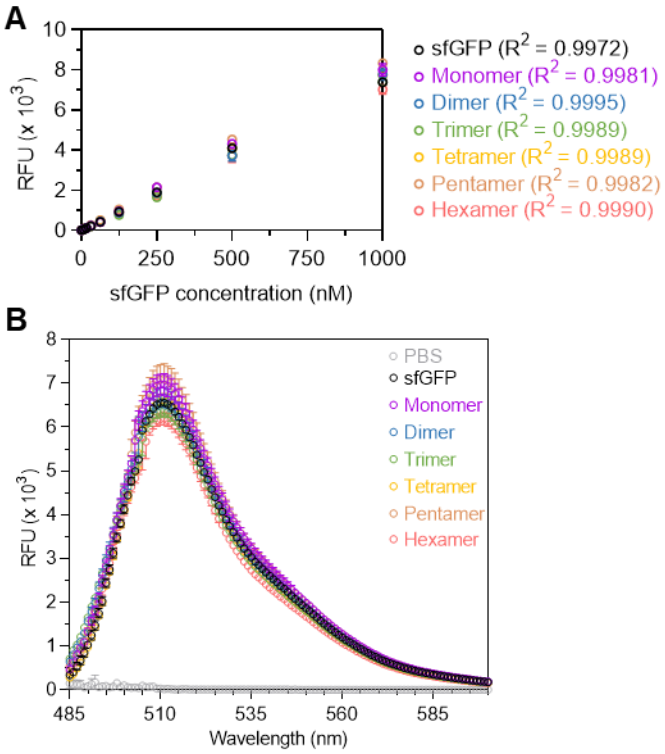

Fig. S4. Fluorescence properties of synthetic Gal3 constructs. (*A*) Standard curve of sfGFP molar concentration versus relative fluorescence units (RFU). (*B*) Fluorescence emission spectra at excitation = 485 nm. For *A* and *B*, *n* = 3, mean ± s.d.

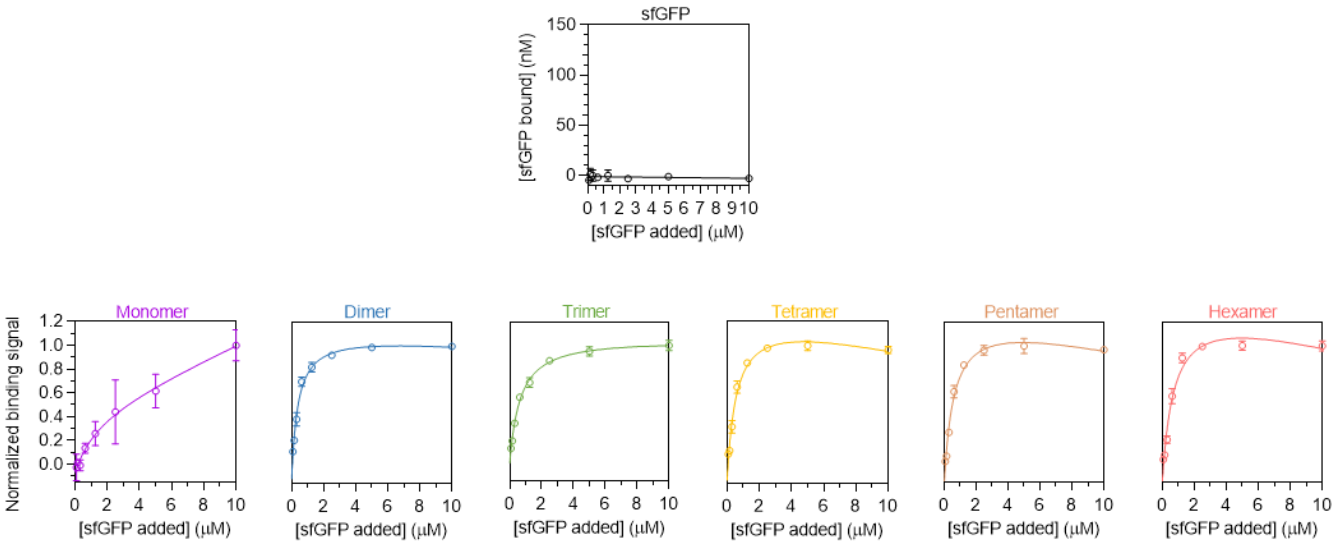

Fig. S5. Saturation binding of protein constructs to surface-adsorbed asialofetuin. *n* = 3, mean ± s.d.

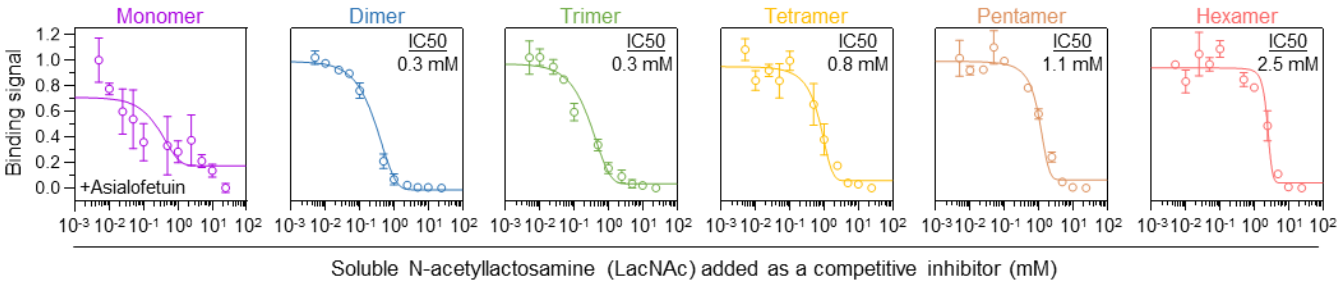

Fig. S6. Competitive binding inhibition of synthetic Gal3 oligomers to immobilized asialofetuin by soluble N-acetyllactosamine (LacNAc). *n* = 3, mean ± s.d. All experiments were performed at an equimolar concentration of sfGFP or Gal3 = 0.5 µM.

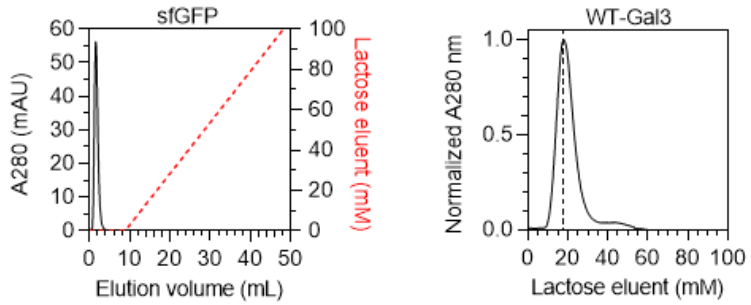

Fig. S7. Lactose affinity chromatography traces of control proteins sfGFP (left) and wild-type-Gal3 (WT-Gal3, right).

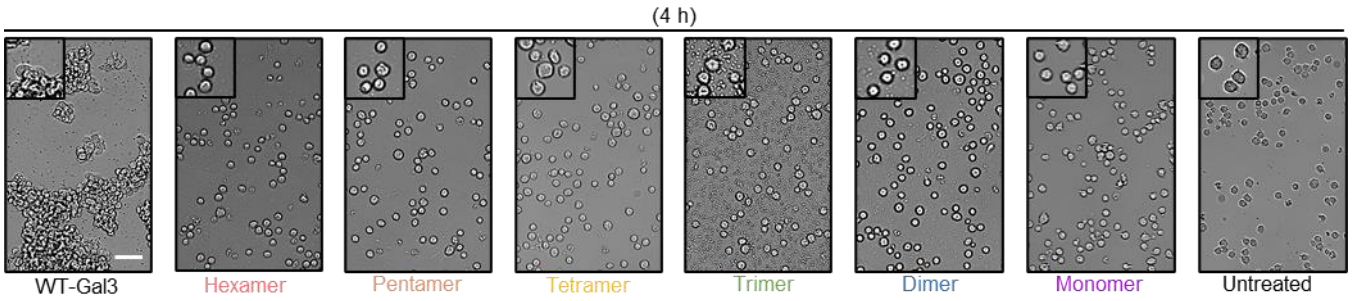

Fig. S8. Brightfield microscopic images taken of Jurkat T cells after 4 h incubation with synthetic Gal3 constructs, wild-type Gal3 (WT-Gal3), or PBS (untreated control). Scale bar = 50 µm. All experiments were performed at an equimolar concentration of Gal3 = 5 µM (i.e., [WT-Gal3] = 5 µM, [Monomer] = 5 µM, [Dimer] = 2.5 µM, [Trimer] = 1.67 µM, [Tetramer] = 1.25 µM, [Pentamer] = 1 µM, [Hexamer] = 0.83 µM).

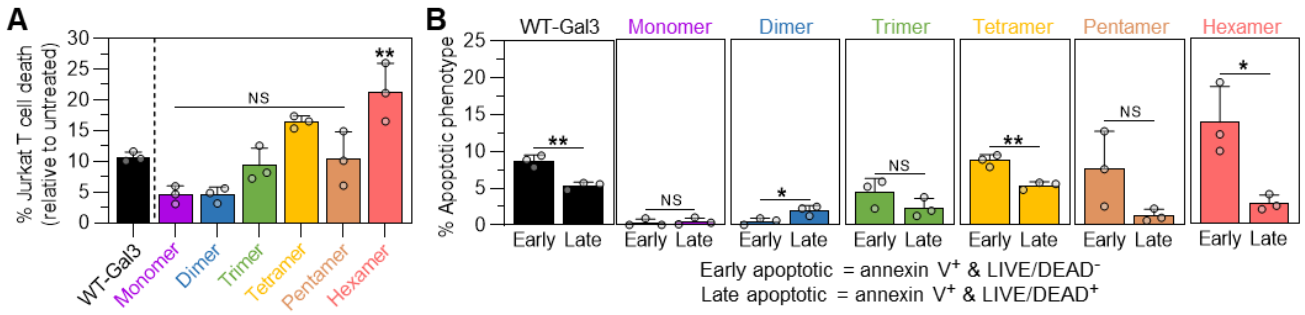

Fig. S9. Cell death signaling activities of synthetic Gal3 constructs. (*A*) Percentage of Jurkat T cell death after 4 h treatment with synthetic Gal3 constructs or wild-type Gal3 (WT-Gal3) relative to PBS-treated cells (untreated control). (*B*) Percentage of Jurkat T cells in the early apoptotic and late apoptotic populations after 4 h treatment with synthetic Gal3 constructs or WT-Gal3, shown relative to the untreated control. For *A*, $n = 3$, mean ± s.d., $^{**}p < 0.01$, NS is no significant difference, and comparisons were made using one-way ANOVA with Tukey's *post hoc*. Statistical comparisons relative to WT-Gal3 are denoted by * or NS symbol. For *B*, $n = 3$, mean ± s.d., $^{*}p < 0.05$, $^{**}p < 0.01$, NS is no significant difference, and comparisons were made using unpaired two-tailed Student's t-test. All experiments were performed at an equimolar concentration of Gal3 = 5 μM (i.e., [WT-Gal3] = 5 μM, [Monomer] = 5 μM, [Dimer] = 2.5 μM, [Trimer] = 1.67 μM, [Tetramer] = 1.25 μM, [Pentamer] = 1 μM, [Hexamer] = 0.83 μM).

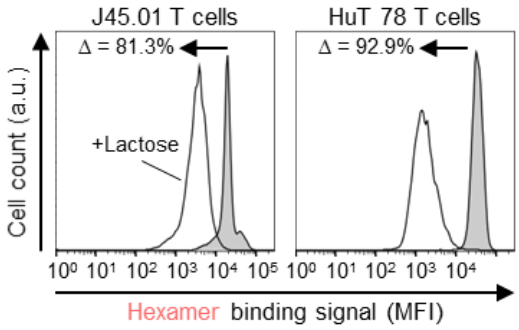

Fig. S10. Competitive inhibition of Hexamer binding to J45.01 (left) and HuT 78 (right) T cells by 100 mM soluble β-lactose. Binding to cells was measured via flow cytometry. Percentages shown represent the change in mean fluorescence intensity (MFI) of cells after the soluble β-lactose wash (white fill) relative to the PBS wash (gray fill). Histograms shown represent one of three replicates per group while the percentages shown are averages of all three replicates. Experiments were performed at a concentration of Gal3 = 5 μM (i.e., [Hexamer] = 0.83 μM).

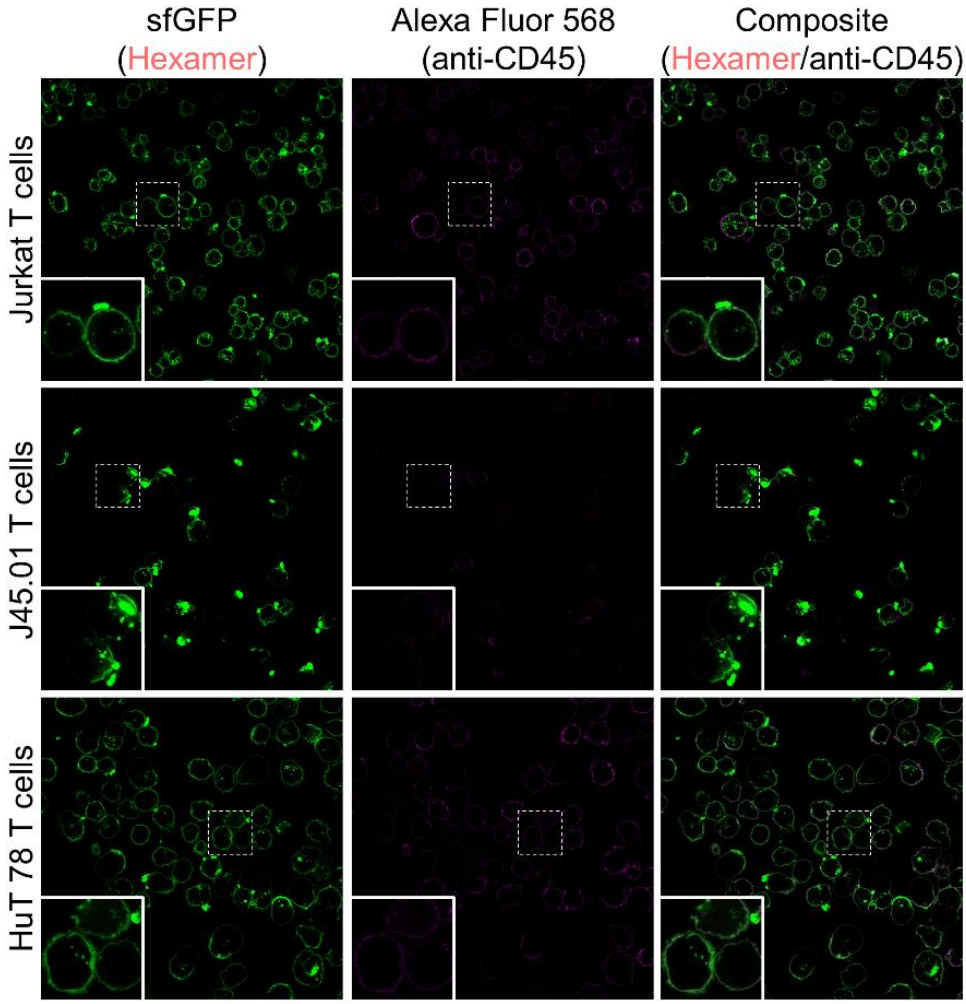

Fig. S11. Confocal microscopic images of Hexamer (green) and CD45 (magenta) on Jurkat, J45.01, and HuT 78 T cells following Hexamer treatment for 2 h.

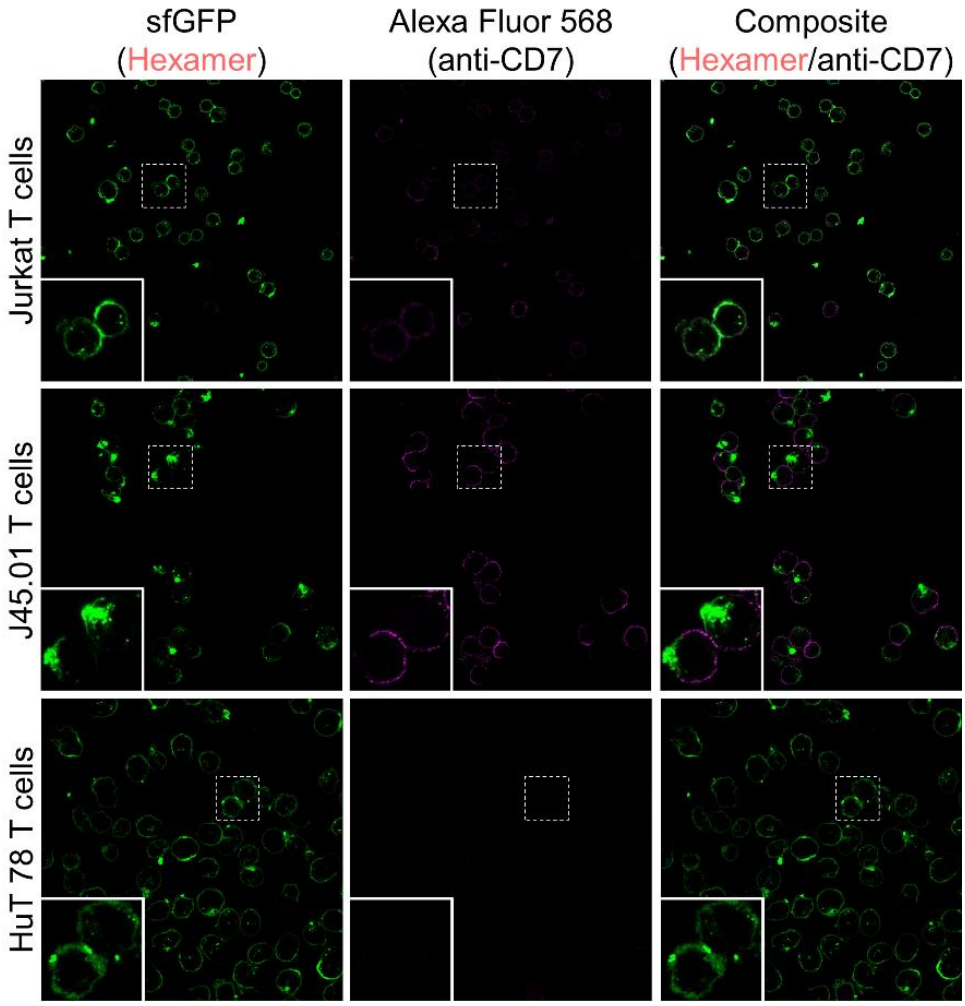

Fig. S12. Confocal microscopic images of Hexamer (green) and CD7 (magenta) on Jurkat, J45.01, and HuT 78 T cells following Hexamer treatment for 2 h.

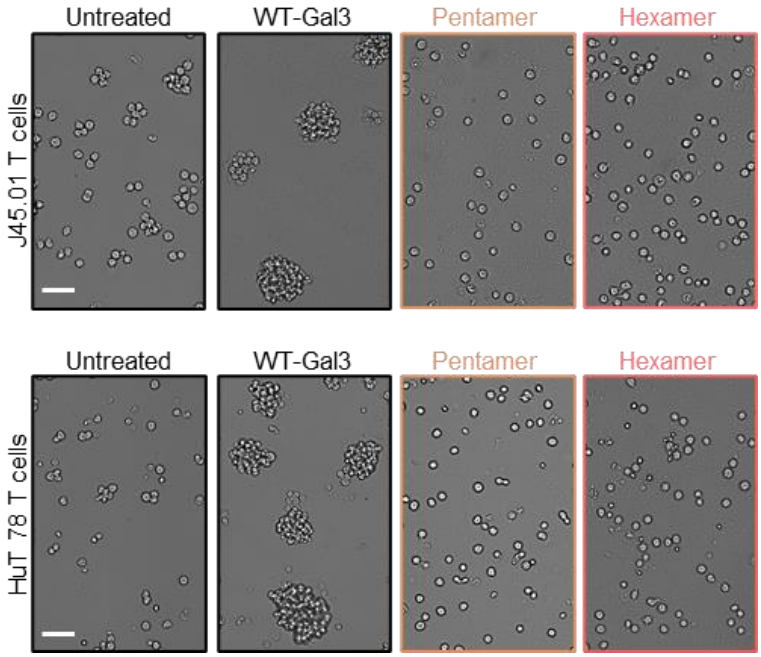

Fig. S13. Brightfield microscopic images taken of J45.01 (top) and HuT 78 (bottom) T cells after 18 h incubation with synthetic Gal3 oligomers, wild-type Gal3 (WT-Gal3), or PBS (untreated control). Scale bar = 50 µm. All experiments were performed at an equimolar concentration of Gal3 = 5 µM (i.e., [WT-Gal3] = 5 µM, [Pentamer] = 1 µM, [Hexamer] = 0.83 µM).

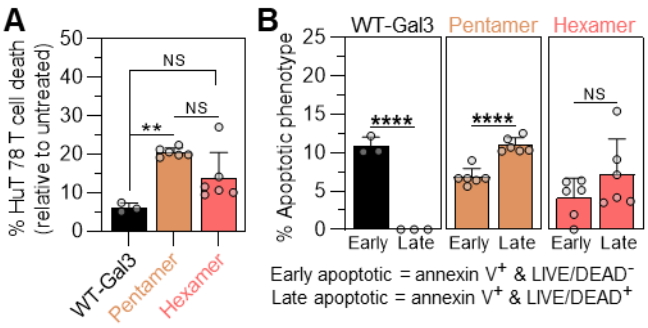

Fig. S14. CD7 regulates cell death signaling activity of wild-type Gal3 and synthetic Gal3 oligomers. (*A*) Percentage of HuT 78 T cell death after 18 h treatment with synthetic galectin-3 oligomers or wild-type galectin-3 (WT-Gal3), shown relative to PBS-treated cells (untreated control). (*B*) Percentage of HuT 78 T cells in the early apoptotic or late apoptotic population after 18 h treatment with synthetic Gal3 oligomers or WT-Gal3 relative to the untreated control. For *A*, $n \geq 3$, mean ± s.d., $^{**}p < 0.01$, NS is no significant difference, and comparisons were made using one-way ANOVA with Tukey's *post hoc*. For *B*, $n \geq 3$, mean ± s.d., $^{****}p < 0.0001$, NS is no significant difference, and comparisons were made using unpaired two-tailed Student's *t*-test. All experiments were performed at an equimolar concentration of Gal3 = 5 μM (i.e., [WT-Gal3] = 5 μM, [Pentamer] = 1 μM, [Hexamer] = 0.83 μM).

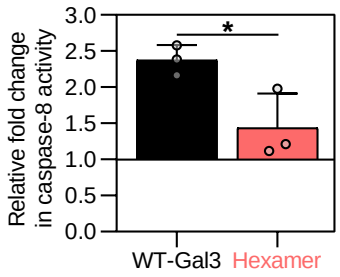

Fig. S15. Fold change in caspase-8 activity of Jurkat T cells treated with wild-type Gal3 (WT-Gal3) or Hexamer, shown relative to PBS-treated cells (untreated control). $n = 3$, mean ± s.d., $*p < 0.05$, and comparisons were made using unpaired two-tailed Student's *t*-test. This experiment was performed at an equimolar concentration of Gal3 = 5 μM (i.e., [WT-Gal3] = 5 μM and [Hexamer] = 0.83 μM).

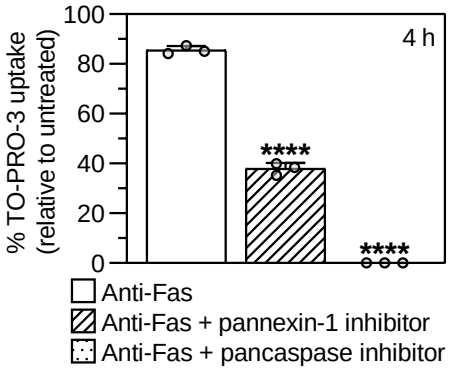

Fig. S16. Percentage of TO-PRO-3 uptake by Jurkat T cells after 4 h treatment with anti-Fas (positive control) in the presence and absence of a pannexin-1 inhibitor or pancaspase inhibitor. *n* = 3, mean ± s.d., ****$p < 0.0001$, NS is no significant difference, and comparisons were made using one-way ANOVA with Tukey's *post hoc*.

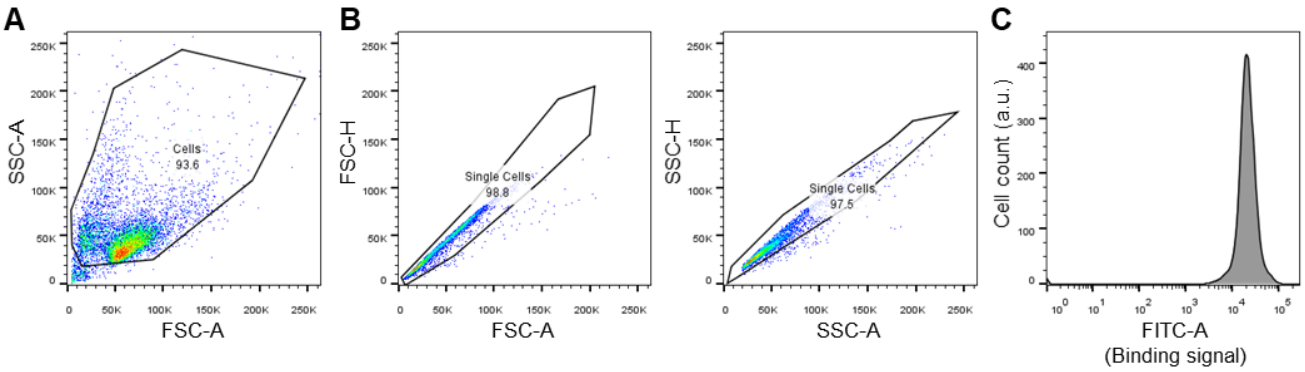

Fig. S17. Flow cytometry gating strategy for analysis of synthetic Gal3 oligomer cell-binding. (*A*) Cells (e.g., Jurkat, J45.01, or HuT 78 T cells) are first gated via FSC-A/SSC-A to remove debris, followed by (*B*) linear gating of single cells via FSC-A/FSC-H and SSC-A/SSC-H prior to (*C*) transforming data into histograms (cell count versus binding signal).

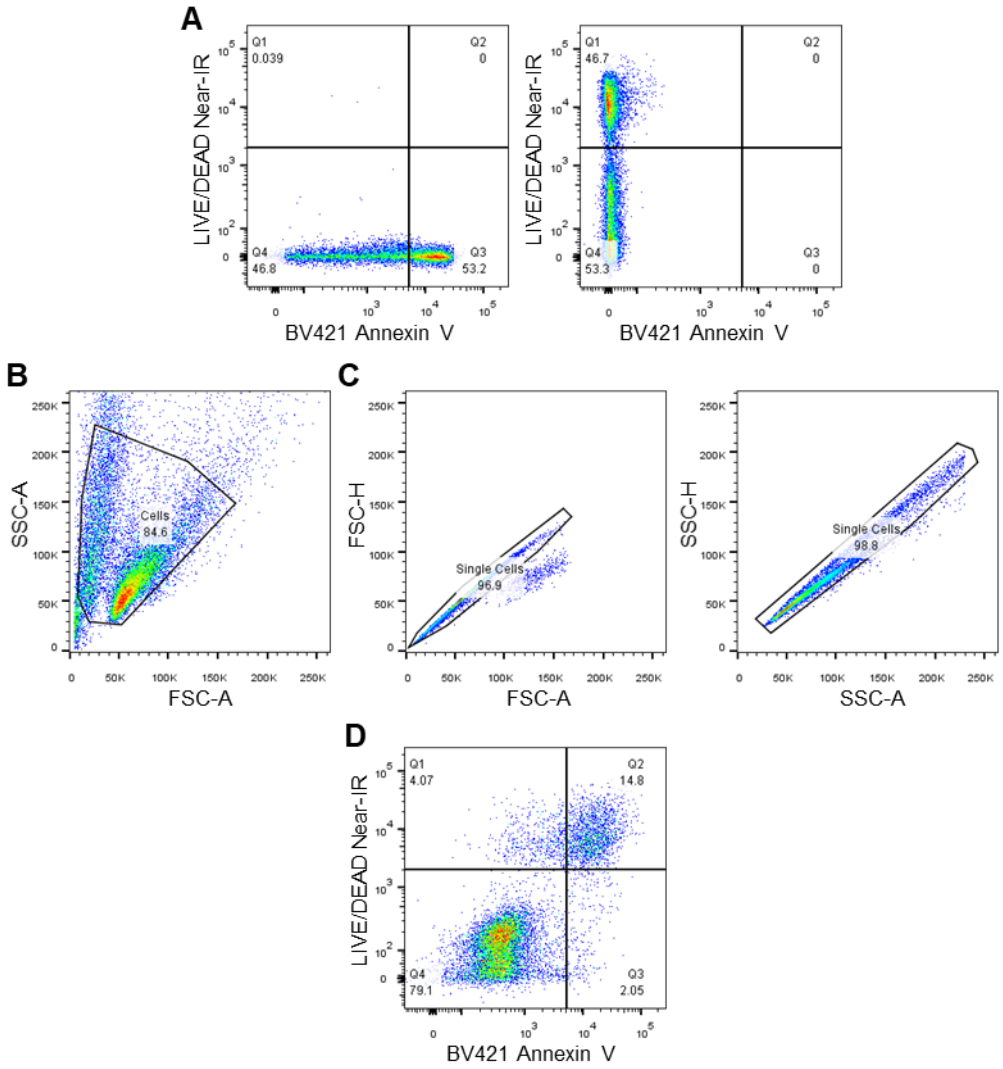

Fig. S18. Flow cytometry gating strategy for analysis of cell death induced by synthetic Gal3 oligomers. (*A*) First, compensation is performed using single stain controls (e.g., sfGFP signal represented by FITC detection with filters 530/30, BV421 detection with filters 450/40, and LIVE/DEAD near-IR represented by APC-Cy™7 with filters 780/60). (*B*) Cells (e.g., Jurkat, J45.01, or HuT 78 T cells) are then gated via FSC-A/SSC-A to remove debris, followed by (*C*) linear gating of single cells via FSC-A/FSC-H and SSC-A/SSC-H prior to (*D*) plotting scatter plots (LIVE/DEAD Near-IR versus BV421 Annexin V). Percentages representing cell death were extrapolated from these scatter plots, as described in the Methods.

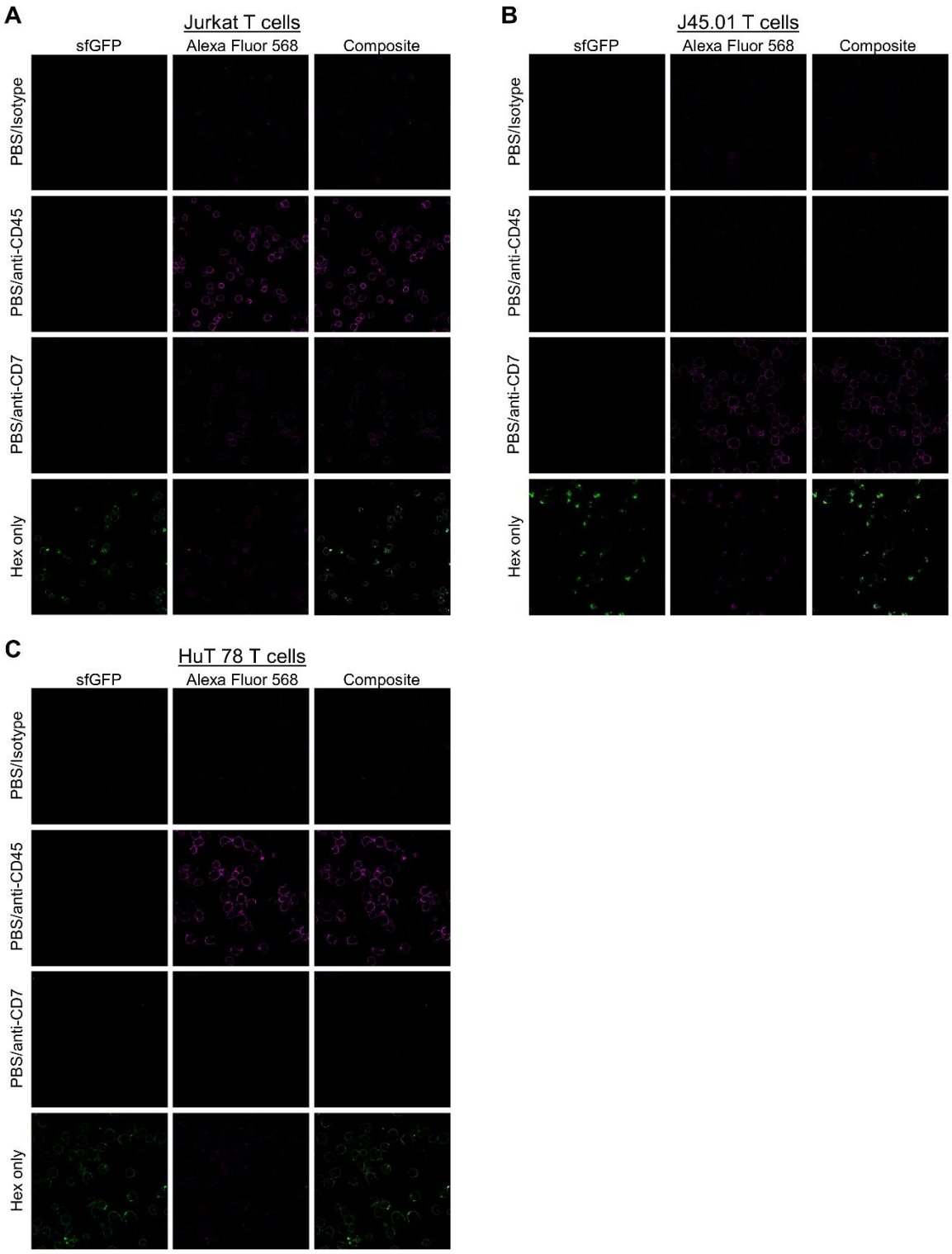

Fig. S19. Confocal microscopic images of isotype and single stain (CD45/CD7) controls following Hexamer or PBS treatment of (*A*) Jurkat, (*B*) J45.01, and (*C*) HuT 78 T cells for 2 h.

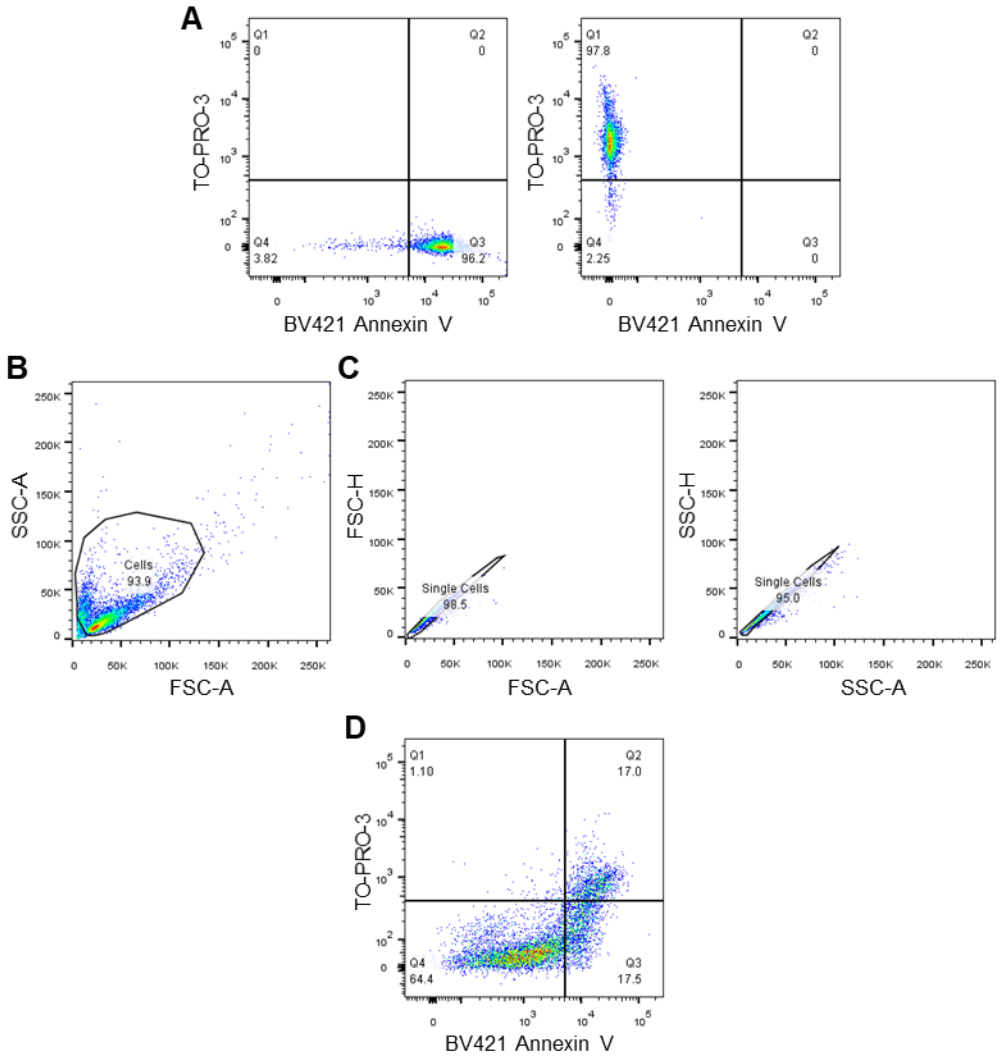

Fig. S20. Flow cytometry gating strategy for analysis of TO-PRO-3 uptake within Jurkat T cells after treatment with wild-type Gal3 or synthetic Gal3 oligomers. (*A*) First, compensation is performed using single stain controls (e.g., sfGFP signal represented by FITC detection with filters 530/30, BV421 detection with filters 450/40, and TO-PRO-3 represented by APC with filters 670/30). (*B*) Jurkat T cells are then gated via FSC-A/SSC-A to remove debris, followed by (*C*) linear gating of single cells via FSC-A/FSC-H and SSC-A/SSC-H prior to (*D*) plotting scatter plots (TO-PRO-3 versus BV421 Annexin V). Percentages representing TO-PRO-3 uptake were extrapolated from these scatter plots, as described in the Methods.

Note S1. Genetic sequences

sfGFP genetic sequence:
CCATGGCGAGCAAGGGTGAAGAACTGTTTACCGGCGTGGTGCCGATCCTGGTGGAGCTGG
ACGGCGATGTGAACGGTCATAAGTTTAGCGTGCGTGGTGAGGGCGAAGGTGACGCGACCA
TCGGCAAGCTGACCCTGAAATTCATTTGCACCACCGGTAAACTGCCGGTGCCGTGGCCGAC
CCTGGTTACCACCCTGACCTACGGCGTGCAGTGCTTTAGCCGTTATCCGGACCACATGAAG
CGTCACGATTTCTTTAAAAGCGCGATGCCGGAGGGCTACGTTCAAGAACGTACCATCAGCTT
CAAGGACGATGGCAAGTATAAAACCCGTGCGGTGGTTAAATTTGAGGGCGACACCCTGGTG
AACCGTATCGAGCTGAAGGGTACCGACTTCAAAGAAGATGGCAACATTCTGGGTCACAAGC
TGGAATACAACTTTAACAGCCACAACGTGTATATCACCGCGGATAAGCAGAAAAACGGCATT
AAAGCGAACTTCACCGTGCGTCACAACGTTGAGGACGGTAGCGTTCAACTGGCGGATCACT
ACCAGCAAAACACCCCGATTGGTGATGGTCCGGTGCTGCTGCCGGATAACCACTATCTGAG
CACCCAGACCGTTCTGAGCAAGGACCCGAACGAAAAACGTGATCACATGGTTCTGCACGAA
TATGTGAATGCGGCGGGTATCACCCTGGGTATGGACGAACTGTATAAACTCGAGCACCACC
ACCACCACCAC

WT-Gal3 genetic sequence:
CCATGGCAGACAATTTTTCGCTCCATGATGCGTTATCTGGGTCTGGAAACCCAAACCCTCAA
GGATGGCCTGGCGCATGGGGGAACCAGCCTGCTGGGGCAGGGGGCTACCCAGGGGCTTC
CTATCCTGGGGCCTACCCCGGGCAGGCACCCCCAGGGGCTTATCCTGGACAGGCACCTCC
AGGCGCCTACCCTGGAGCACCTGGAGCTTATCCCGGAGCACCTGCACCTGGAGTCTACCCA
GGGCCACCCAGCGGCCCTGGGGCCTACCCATCTTCTGGACAGCCAAGTGCCCCCGGAGCC
TACCCTGCCACTGGCCCCTATGGCGCCCCTGCTGGGCCACTGATTGTGCCTTATAACCTGC
CTTTGCCTGGGGGAGTGGTGCCTCGCATGCTGATAACAATTCTGGGCACGGTGAAGCCCAA
TGCAAACAGAATTGCTTTAGATTTCCAAAGAGGGAATGATGTTGCCTTCCACTTTAACCCACG
CTTCAATGAGAACAACAGGAGAGTCATTGTTTGCAATACAAAGCTGGATAATAACTGGGGAA
GGGAAGAAAGACAGTCGGTTTTCCCATTTGAAAGTGGGAAACCATTCAAAATACAAGTACTG
GTTGAACCTGACCACTTCAAGGTTGCAGTGAATGATGCTCACTTGTTGCAGTACAATCATCG
GGTTAAAAAACTCAATGAAATCAGCAAACTGGGAATTTCTGGTGACATAGACCTCACCAGTG
CTTCATATAACATGATACTCGAGCACCACCACCACCAC

Monomer genetic sequence:
CCATGTCCAAAGGAGAAGAGCTGTTCACTGGAGTGGTACCAATACTTGTGGAGTTGGACGG
AGATGTGAACGGACACAAATTTTCAGTCCGCGGGGAGGGGGAAGGGGATGCTACTATTGGC
AAGCTGACGCTCAAATTCATCTGTACCACCGGAAAACTCCCTGTACCCTGGCCCACACTGGT
GACAACTCTGACTTACGGCGTGCAATGTTTTAGCCGATACCCAGACCACATGAAGAGGCAC
GACTTTTTCAAAAGCGCAATGCCTGAAGGATACGTACAGGAAAGGACCATTTCTTTTAAAGA
CGACGGGAAGTACAAAACCCGGGCAGTGGTGAAGTTTGAGGGCGATACCCTCGTCAATAGG
ATCGAATTGAAGGGAACTGACTTCAAAGAAGATGGCAACATCCTGGGTCACAAGCTTGAGTA
TAACTTTAACTCCCACAACGTGTATATTACAGCCGACAAACAGAAGAATGGAATTAAGGCTAA
CTTCACTGTCAGACACAATGTCGAAGATGGCTCCGTGCAGCTCGCCGATCACTATCAACAGA
ATACTCCTATCGGGGACGGCCCAGTCCTGCTGCCCGACAACCACTACCTGAGTACCCAGAC
TGTTCTGAGCAAAGATCCGAACGAGAAGCGCGACCACATGGTGCTGCATGAGTATGTCAAC
GCTGCGGGAATTACCCTCGGCATGGACGAGCTGTACAAGGGATCCGGCGGCGGCAGCGGC
GGCAGCGGCGGCAGCGGCGGCGAATTCGCAGACAATTTTTCGCTCCATGATGCGTTATCTG
GGTCTGGAAACCCAAACCCTCAAGGATGGCCTGGCGCATGGGGGAACCAGCCTGCTGGGG
CAGGGGGCTACCCAGGGGCTTCCTATCCTGGGGCCTACCCCGGGCAGGCACCCCCAGGG
GCTTATCCTGGACAGGCACCTCCAGGCGCCTACCCTGGAGCACCTGGAGCTTATCCCGGAG
CACCTGCACCTGGAGTCTACCCAGGGCCACCCAGCGGCCCTGGGGCCTACCCATCTTCTG
GACAGCCAAGTGCCCCCGGAGCCTACCCTGCCACTGGCCCCTATGGCGCCCCTGCTGGGC
CACTGATTGTGCCTTATAACCTGCCTTTGCCTGGGGGAGTGGTGCCTCGCATGCTGATAACA
ATTCTGGGCACGGTGAAGCCCAATGCAAACAGAATTGCTTTAGATTTCCAAAGAGGGAATG7
5ATGTTGCCTTCCACTTTAACCCACGCTTCAATGAGAACAACAGGAGAGTCATTGTTTGCAAT
ACAAAGCTGGATAATAACTGGGGAAGGGAAGAAAGACAGTCGGTTTTCCCATTTGAAAGTGG
GAAACCATTCAAAATACAAGTACTGGTTGAACCTGACCACTTCAAGGTTGCAGTGAATGATG

CTCACTTGTTGCAGTACAATCATCGGGTTAAAAAACTCAATGAAATCAGCAAACTGGGAATTT
CTGGTGACATAGACCTCACCAGTGCTTCATATAACATGATACTCGAGCACCACCACCACCAC
CAC

Dimer (coiled-coil: 'GCN4-pM1') genetic sequence:
CCATGGCGAGCAAGGGCGAGGAACTGTTCACCGGTGTGGTTCCGATCCTGGTGGAGCTGG
ACGGCGATGTTAACGGTCACAAATTTAGCGTGCGTGGCGAGGGTGAAGGCGACGCGACCA
TCGGCAAGCTGACCCTGAAATTCATTTGCACCACCGGTAAGCTGCCGGTGCCGTGGCCGAC
CCTGGTTACCACCCTGACCTACGGTGTGCAGTGCTTTAGCCGTTATCCGGACCACATGAAG
CGTCACGATTTCTTTAAAAGCGCGATGCCGGAGGGCTACGTTCAAGAACGTACCATTAGCTT
CAAGGACGATGGTAAGTATAAAACCCGTGCGGTGGTTAAATTTGAGGGCGACACCCTGGTT
AACCGTATCGAGCTGAAGGGTACCGACTTCAAAGAAGATGGCAACATTCTGGGTCACAAGC
TGGAATACAACTTTAACAGCCACAACGTGTATATCACCGCGGATAAGCAGAAAAACGGCATT
AAAGCGAACTTCACCGTGCGTCACAACGTTGAGGACGGTAGCGTTCAACTGGCGGATCACT
ACCAGCAAAACACCCCGATCGGTGACGGCCCGGTGCTGCTGCCGGATAACCACTATCTGAG
CACCCAGACCGTTCTGAGCAAGGACCCGAACGAGAAACGTGATCACATGGTGCTGCACGAA
TACGTTAACGCGGCGGGCATTACCCTGGGTATGGACGAACTGTATAAAGGTGGCGGTAGCG
GCGGTAGCGGCGGTAGCGGCGGTGGATCCATGGCGCGTATGAAGCAACTGGAGGATCGTG
TGGAGGAACTGGAAAGCAAAAACTACCACCTGGAGAACGAAGTGGCGCGTCTGAAGAAACT
GGTTGGTGAGCGTGAATTCGGTGGCGGTAGCGGCGGTAGCGGCGGTGGCGGTAGCGGCG
GTAGCGGTGCGGACAACTTCAGCCTGCACGATGCGCTGAGCGGTAGCGGCAACCCGAACC
CGCAGGGTTGGCCGGGCGCGTGGGGTAACCAACCGGCGGGCGCGGGCGGTTACCCGGGT
GCGAGCTACCCGGGCGCGTATCCGGGTCAGGCGCCGCCGGGCGCGTATCCGGGTCAAGC
GCCGCCGGGCGCGTACCCGGGCGCGCCGGGTGCGTATCCGGGTGCGCCGGCGCCGGGC
GTGTACCCGGGTCCGCCGAGCGGTCCGGGCGCGTATCCGAGCAGCGGCCAGCCGAGCGC
GCCGGGTGCGTACCCGGCGACCGGCCCGTATGGTGCGCCGGCGGGTCCGCTGATCGTTC
CGTACAACCTGCCGCTGCCGGGCGGTGTGGTTCCGCGTATGCTGATCACCATTCTGGGTAC
CGTGAAGCCGAACGCGAACCGTATCGCGCTGGACTTCCAACGTGGTAACGATGTTGCGTTC
CACTTTAACCCGCGTTTTAACGAAAACAACCGTCGTGTGATTGTTTGCAACACCAAACTGGA
CAACAACTGGGGCCGTGAGGAACGTCAGAGCGTGTTCCCGTTTGAGAGCGGTAAGCCGTTC
AAAATCCAAGTGCTGGTTGAACCGGACCACTTTAAGGTGGCGGTTAACGATGCGCACCTGC
TGCAGTACAACCACCGTGTTAAGAAACTGAACGAGATCAGCAAACTGGGCATCAGCGGTGA
CATTGATCTGACCAGCGCGAGCTATAACATGATTCTGGAACACCACCACCACCACCAC

Trimer (coiled-coil: 'GCN4-pM3') genetic sequence:
CCATGTCCAAAGGAGAAGAGCTGTTCACTGGAGTGGTACCAATACTTGTGGAGTTGGACGG
AGATGTGAACGGACACAAATTTTCAGTCCGCGGGGAGGGGGAAGGGGATGCTACTATTGGC
AAGCTGACGCTCAAATTCATCTGTACCACCGGAAAACTCCCTGTACCCTGGCCCACACTGGT
GACAACTCTGACTTACGGCGTGCAATGTTTTAGCCGATACCCAGACCACATGAAGAGGCAC
GACTTTTTCAAAAGCGCAATGCCTGAAGGATACGTACAGGAAAGGACCATTTCTTTTAAAGA
CGACGGGAAGTACAAAACCCGGGCAGTGGTGAAGTTTGAGGGCGATACCCTCGTCAATAGG
ATCGAATTGAAGGGAACTGACTTCAAAGAAGATGGCAACATCCTGGGTCACAAGCTTGAGTA
TAACTTTAACTCCCACAACGTGTATATTACAGCCGACAAACAGAAGAATGGAATTAAGGCTAA
CTTCACTGTCAGACACAATGTCGAAGATGGCTCCGTGCAGCTCGCCGATCACTATCAACAGA
ATACTCCTATCGGGGACGGCCCAGTCCTGCTGCCCGACAACCACTACCTGAGTACCCAGAC
TGTTCTGAGCAAAGATCCGAACGAGAAGCGCGACCACATGGTGCTGCATGAGTATGTCAAC
GCTGCGGGAATTACCCTCGGCATGGACGAGCTGTACAAGGGATCCGGCGGCGGCAGCGGC
GGCAGCGGCGGCAGCGGCGGCATGGCGCGCATGAAACAGCTGGAAGATAAAGTGGAAGAA
CTGCTGAGCAAAAACTATCATCTGGAAAACCGCGTGGCGCGCCTGGAAAAACTGGTGGGCG
AACGCGGCGGCGGCAGCGGCGGCAGCGGCGGCGGCGGCAGCGGCGGCAGCGGCGAATT
CGCAGACAATTTTTCGCTCCATGATGCGTTATCTGGGTCTGGAAACCCAAACCCTCAAGGAT
GGCCTGGCGCATGGGGGAACCAGCCTGCTGGGGCAGGGGGCTACCCAGGGGCTTCCTAT
CCTGGGGCCTACCCCGGGCAGGCACCCCCAGGGGCTTATCCTGGACAGGCACCTCCAGGC
GCCTACCCTGGAGCACCTGGAGCTTATCCCGGAGCACCTGCACCTGGAGTCTACCCAGGG
CCACCCAGCGGCCCTGGGGCCTACCCATCTTCTGGACAGCCAAGTGCCCCCGGAGCCTAC
CCTGCCACTGGCCCCTATGGCGCCCCTGCTGGGCCACTGATTGTGCCTTATAACCTGCCTT

TGCCTGGGGGAGTGGTGCCTCGCATGCTGATAACAATTCTGGGCACGGTGAAGCCCAATGC
AAACAGAATTGCTTTAGATTTCCAAAGAGGGAATGATGTTGCCTTCCACTTTAACCCACGCTT
CAATGAGAACAACAGGAGAGTCATTGTTTGCAATACAAAGCTGGATAATAACTGGGGAAGGG
AAGAAAGACAGTCGGTTTTCCCATTTGAAAGTGGGAAACCATTCAAAATACAAGTACTGGTT
GAACCTGACCACTTCAAGGTTGCAGTGAATGATGCTCACTTGTTGCAGTACAATCATCGGGT
TAAAAAACTCAATGAAATCAGCAAACTGGGAATTTCTGGTGACATAGACCTCACCAGTGCTTC
ATATAACATGATACTCGAGCACCACCACCACCACCAC

Tetramer (coiled-coil: ‘GCN4-pLI) genetic sequence:
CCATGGCGAGCAAGGGCGAGGAACTGTTCACCGGTGTGGTTCCGATCCTGGTGGAGCTGG
ACGGCGATGTTAACGGTCACAAATTTAGCGTGCGTGGCGAGGGTGAAGGCGACGCGACCA
TCGGCAAGCTGACCCTGAAATTCATTTGCACCACCGGTAAGCTGCCGGTGCCGTGGCCGAC
CCTGGTTACCACCCTGACCTACGGTGTGCAGTGCTTTAGCCGTTATCCGGACCACATGAAG
CGTCACGATTTCTTTAAAAGCGCGATGCCGGAGGGCTACGTTCAAGAACGTACCATTAGCTT
CAAGGACGATGGTAAGTATAAAACCCGTGCGGTGGTTAAATTTGAGGGCGACACCCTGGTT
AACCGTATCGAGCTGAAGGGTACCGACTTCAAAGAAGATGGCAACATTCTGGGTCACAAGC
TGGAATACAACTTTAACAGCCACAACGTGTATATCACCGCGGATAAGCAGAAAAACGGCATT
AAAGCGAACTTCACCGTGCGTCACAACGTTGAAGACGGTAGCGTTCAACTGGCGGATCACT
ACCAGCAAAACACCCCGATCGGTGACGGCCCGGTGCTGCTGCCGGATAACCACTATCTGAG
CACCCAGACCGTTCTGAGCAAGGACCCGAACGAGAAACGTGATCACATGGTGCTGCACGAA
TACGTTAACGCGGCGGGCATTACCCTGGGTATGGACGAGCTGTATAAGGGTGGCGGTAGC
GGCGGTAGCGGCGGTAGCGGCGGTGGATCCATGGCGCGTATGAAGCAAATCGAAGATAAA
CTGGAGGAAATTCTGAGCAAACTGTACCACATCGAGAACGAACTGGCGCGTATTAAGAAACT
GCTGGGTGAGCGTGAATTCGGTGGCGGTAGCGGCGGTAGCGGCGGTGGCGGTAGCGGCG
GTAGCGGTGCGGACAACTTCAGCCTGCACGATGCGCTGAGCGGTAGCGGCAACCCGAACC
CGCAGGGTTGGCCGGGCGCGTGGGGTAACCAACCGGCGGGCGCGGGCGGTTACCCGGGT
GCGAGCTACCCGGGCGCGTATCCGGGTCAGGCGCCGCCGGGCGCGTATCCGGGTCAAGC
GCCGCCGGGCGCGTACCCGGGCGCGCCGGGTGCGTATCCGGGTGCGCCGGCGCCGGGC
GTGTACCCGGGTCCGCCGAGCGGTCCGGGCGCGTATCCGAGCAGCGGCCAGCCGAGCGC
GCCGGGTGCGTACCCGGCGACCGGCCCGTATGGTGCGCCGGCGGGTCCGCTGATCGTTC
CGTACAACCTGCCGCTGCCGGGCGGTGTGGTTCCGCGTATGCTGATCACCATTCTGGGTAC
CGTGAAGCCGAACGCGAACCGTATCGCGCTGGACTTCCAACGTGGTAACGATGTTGCGTTC
CACTTTAACCCGCGTTTTAACGAGAACAACCGTCGTGTGATTGTTTGCAACACCAAACTGGA
CAACAACTGGGGCCGTGAGGAACGTCAGAGCGTGTTCCCGTTTGAGAGCGGTAAGCCGTTC
AAAATCCAAGTGCTGGTTGAACCGGACCACTTTAAGGTGGCGGTTAACGATGCGCACCTGC
TGCAGTACAACCACCGTGTTAAGAAACTGAACGAGATCAGCAAACTGGGCATCAGCGGTGA
CATTGATCTGACCAGCGCGAGCTATAACATGATTCTGGAACACCACCACCACCACCAC

Pentamer (coiled-coil: ‘CC-Pent’) genetic sequence:
CCATGGCGTCCAAAGGAGAAGAGCTGTTCACTGGAGTGGTACCAATACTTGTGGAGTTGGA
CGGAGATGTGAACGGACACAAATTTTCAGTCCGCGGGGAGGGGGAAGGGGATGCTACTATT
GGCAAGCTGACGCTCAAATTCATCTGTACCACCGGAAAACTCCCTGTACCCTGGCCCACACT
GGTGACAACTCTGACTTACGGCGTGCAATGTTTTAGCCGATACCCAGACCACATGAAGAGG
CACGACTTTTTCAAAAGCGCAATGCCTGAAGGATACGTACAGGAAAGGACCATTTCTTTTAAA
GACGACGGGAAGTACAAAACCCGGGCAGTGGTGAAGTTTGAGGGCGATACCCTCGTCAATA
GGATCGAATTGAAGGGAACTGACTTCAAAGAAGATGGCAACATCCTGGGTCACAAGCTTGA
GTATAACTTTAACTCCCACAACGTGTATATTACAGCCGACAAACAGAAGAATGGAATTAAGGC
TAACTTCACTGTCAGACACAATGTCGAAGATGGCTCCGTGCAGCTCGCCGATCACTATCAAC
AGAATACTCCTATCGGGGACGGCCCAGTCCTGCTGCCCGACAACCACTACCTGAGTACCCA
GACTGTTCTGAGCAAAGATCCGAACGAGAAGCGCGACCACATGGTGCTGCATGAGTATGTC
AACGCTGCGGGAATTACCCTCGGCATGGACGAGCTGTACAAGGGGGGGGGTAGTGGAGGA
TCGGGCGGCTCTGGAGGTGGATCCGGCAAGATCGAACAGATTCTGCAGAAGATTGAAAAAA
TTTTGCAAAAGATCGAATGGATTCTTCAGAAAATCGAACAAATTTTACAGGGCGAATTCGGTG
GTGGGTCGGGCGGGTCTGGCGGCGGCGGATCTGGTGGATCTGGCGCAGACAATTTTTCGC
TCCATGATGCGTTATCTGGGTCTGGAAACCCAAACCCTCAAGGATGGCCTGGCGCATGGGG
GAACCAGCCTGCTGGGGCAGGGGGCTACCCAGGGGCTTCCTATCCTGGGGCCTACCCCGG

GCAGGCACCCCCAGGGGCTTATCCTGGACAGGCACCTCCAGGCGCCTACCCTGGAGCACC
TGGAGCTTATCCCGGAGCACCTGCACCTGGAGTCTACCCAGGGCCACCCAGCGGCCCTGG
GGCCTACCCATCTTCTGGACAGCCAAGTGCCCCCGGAGCCTACCCTGCCACTGGCCCCTAT
GGCGCCCCTGCTGGGCCACTGATTGTGCCTTATAACCTGCCTTTGCCTGGGGGAGTGGTGC
CTCGCATGCTGATAACAATTCTGGGCACGGTGAAGCCCAATGCAAACAGAATTGCTTTAGAT
TTCCAAAGAGGGAATGATGTTGCCTTCCACTTTAACCCACGCTTCAATGAGAACAACAGGAG
AGTCATTGTTTGCAATACAAAGCTGGATAATAACTGGGGAAGGGAAGAAAGACAGTCGGTTT
TCCCATTTGAAAGTGGGAAACCATTCAAAATACAAGTACTGGTTGAACCTGACCACTTCAAG
GTTGCAGTGAATGATGCTCACTTGTTGCAGTACAATCATCGGGTTAAAAAACTCAATGAAATC
AGCAAACTGGGAATTTCTGGTGACATAGACCTCACCAGTGCTTCATATAACATGATACTCGA
GCACCACCACCACCACCAC

Hexamer (coiled-coil: 'CC-Hex') genetic sequence:
CCATGGCGAGCAAGGGCGAGGAACTGTTCACCGGTGTGGTTCCGATCCTGGTGGAGCTGG
ACGGCGATGTTAACGGTCACAAATTTAGCGTGCGTGGCGAGGGTGAAGGCGACGCGACCA
TCGGCAAGCTGACCCTGAAATTCATTTGCACCACCGGTAAGCTGCCGGTGCCGTGGCCGAC
CCTGGTTACCACCCTGACCTACGGTGTGCAGTGCTTTAGCCGTTATCCGGACCACATGAAG
CGTCACGATTTCTTTAAAAGCGCGATGCCGGAGGGCTACGTTCAAGAACGTACCATTAGCTT
CAAGGACGATGGTAAGTATAAAACCCGTGCGGTGGTTAAATTTGAGGGCGACACCCTGGTT
AACCGTATCGAGCTGAAGGGTACCGACTTCAAAGAAGATGGCAACATTCTGGGTCACAAGC
TGGAATACAACTTTAACAGCCACAACGTGTATATCACCGCGGATAAGCAGAAAAACGGCATT
AAAGCGAACTTCACCGTGCGTCACAACGTTGAAGACGGTAGCGTTCAACTGGCGGATCACT
ACCAGCAAAACACCCCGATCGGTGACGGCCCGGTGCTGCTGCCGGATAACCACTATCTGAG
CACCCAGACCGTTCTGAGCAAGGACCCGAACGAGAAACGTGATCACATGGTGCTGCACGAA
TACGTTAACGCGGCGGGCATTACCCTGGGTATGGATGAGCTGTATAAGGGTGGCGGTAGCG
GCGGTAGCGGCGGTAGCGGCGGTGGATCCGGTGAGCTGAAGGCGATCGCGCAGGAACTG
AAAGCGATTGCGAAGGAGCTGAAAGCGATCGCGTGGGAACTGAAAGCGATTGCGCAAGGT
GCGGGCGAATTCGGTGGCGGTAGCGGCGGTAGCGGCGGTGGCGGTAGCGGCGGTAGCG
GTGCGGACAACTTCAGCCTGCACGATGCGCTGAGCGGTAGCGGCAACCCGAACCCGCAGG
GTTGGCCGGGCGCGTGGGGTAACCAACCGGCGGGCGCGGGCGGTTACCCGGGTGCGAGC
TACCCGGGCGCGTATCCGGGTCAGGCGCCGCCGGGCGCGTATCCGGGTCAAGCGCCGCC
GGGCGCGTACCCGGGCGCGCCGGGTGCGTATCCGGGTGCGCCGGCGCCGGGCGTGTAC
CCGGGTCCGCCGAGCGGTCCGGGCGCGTATCCGAGCAGCGGCCAGCCGAGCGCGCCGG
GTGCGTACCCGGCGACCGGCCCGTATGGTGCGCCGGCGGGTCCGCTGATCGTTCCGTACA
ACCTGCCGCTGCCGGGCGGTGTGGTTCCGCGTATGCTGATCACCATTCTGGGTACCGTGAA
GCCGAACGCGAACCGTATCGCGCTGGACTTCCAACGTGGTAACGATGTTGCGTTCCACTTT
AACCCGCGTTTTAACGAGAACAACCGTCGTGTGATTGTTTGCAACACCAAACTGGACAACAA
CTGGGGCCGTGAGGAACGTCAGAGCGTGTTCCCGTTTGAGAGCGGTAAGCCGTTCAAAATC
CAAGTGCTGGTTGAACCGGACCACTTTAAGGTGGCGGTTAACGATGCGCACCTGCTGCAGT
ACAACCACCGTGTTAAGAAACTGAACGAGATCAGCAAACTGGGCATCAGCGGTGACATTGAT
CTGACCAGCGCGAGCTACAACATGATTCTGGAACACCACCACCACCACCAC

Note S2. Amino acid sequences

sfGFP amino acid sequence:
MASKGEELFTGVVPILVELDGDVNGHKFSVRGEGEGDATIGKLTLKFICTTGKLPVPWPTLVTTLT
YGVQCFSRYPDHMKRHDFFKSAMPEGYVQERTISFKDDGKYKTRAVVKFEGDTLVNRIELKGTD
FKEDGNILGHKLEYNFNSHNVYITADKQKNGIKANFTVRHNVEDGSVQLADHYQQNTPIGDGPVL
LPDNHYLSTQTVLSKDPNEKRDHMVLHEYVNAAGITLGMDELYKLEHHHHHH

WT-Gal3 amino acid sequence:
MADNFSLHDALSGSGNPNPQGWPGAWGNQPAGAGGYPGASYPGAYPGQAPPGAYPGQAPP
GAYPGAPGAYPGAPAPGVYPGPPSGPGAYPSSGQPSAPGAYPATGPYGAPAGPLIVPYNLPLP
GGVVPRMLITILGTVKPNANRIALDFQRGNDVAFHFNPRFNENNRRVIVCNTKLDNNWGREERQ
SVFPFESGKPFKIQVLVEPDHFKVAVNDAHLLQYNHRVKKLNEISKLGISGDIDLTSASYNMILEHH
HHHH

Monomer amino acid sequence:
MSKGEELFTGVVPILVELDGDVNGHKFSVRGEGEGDATIGKLTLKFICTTGKLPVPWPTLVTTLTY
GVQCFSRYPDHMKRHDFFKSAMPEGYVQERTISFKDDGKYKTRAVVKFEGDTLVNRIELKGTDF
KEDGNILGHKLEYNFNSHNVYITADKQKNGIKANFTVRHNVEDGSVQLADHYQQNTPIGDGPVLL
PDNHYLSTQTVLSKDPNEKRDHMVLHEYVNAAGITLGMDELYKGSGGGSGGGSGGGSGGEFADN
FSLHDALSGSGNPNPQGWPGAWGNQPAGAGGYPGASYPGAYPGQAPPGAYPGQAPPGAYP
GAPGAYPGAPAPGVYPGPPSGPGAYPSSGQPSAPGAYPATGPYGAPAGPLIVPYNLPLPGGVV
PRMLITILGTVKPNANRIALDFQRGNDVAFHFNPRFNENNRRVIVCNTKLDNNWGREERQSVFPF
ESGKPFKIQVLVEPDHFKVAVNDAHLLQYNHRVKKLNEISKLGISGDIDLTSASYNMILEHHHHHH

Dimer (coiled-coil: 'GCN4-pM1') amino acid sequence:
MASKGEELFTGVVPILVELDGDVNGHKFSVRGEGEGDATIGKLTLKFICTTGKLPVPWPTLVTTLT
YGVQCFSRYPDHMKRHDFFKSAMPEGYVQERTISFKDDGKYKTRAVVKFEGDTLVNRIELKGTD
FKEDGNILGHKLEYNFNSHNVYITADKQKNGIKANFTVRHNVEDGSVQLADHYQQNTPIGDGPVL
LPDNHYLSTQTVLSKDPNEKRDHMVLHEYVNAAGITLGMDELYKGGGSGGGSGGGSGGGSMARM
KQLEDRVEELESKNYHLENEVARLKKLVGEREFGGGSGGSGGGGSGGSGADNFSLHDALSGS
GNPNPQGWPGAWGNQPAGAGGYPGASYPGAYPGQAPPGAYPGQAPPGAYPGAPGAYPGAP
APGVYPGPPSGPGAYPSSGQPSAPGAYPATGPYGAPAGPLIVPYNLPLPGGVVPRMLITILGTVK
PNANRIALDFQRGNDVAFHFNPRFNENNRRVIVCNTKLDNNWGREERQSVFPFESGKPFKIQVL
VEPDHFKVAVNDAHLLQYNHRVKKLNEISKLGISGDIDLTSASYNMILEHHHHHH

Trimer (coiled-coil: 'GCN4-pM3') amino acid sequence:
MSKGEELFTGVVPILVELDGDVNGHKFSVRGEGEGDATIGKLTLKFICTTGKLPVPWPTLVTTLTY
GVQCFSRYPDHMKRHDFFKSAMPEGYVQERTISFKDDGKYKTRAVVKFEGDTLVNRIELKGTDF
KEDGNILGHKLEYNFNSHNVYITADKQKNGIKANFTVRHNVEDGSVQLADHYQQNTPIGDGPVLL
PDNHYLSTQTVLSKDPNEKRDHMVLHEYVNAAGITLGMDELYKGSGGGSGGGSGGGSGGGMARMK
QLEDKVEELLSKNYHLENRVARLEKLVGERGGGSGGSGGGGSGGSGEFADNFSLHDALSGSG
NPNPQGWPGAWGNQPAGAGGYPGASYPGAYPGQAPPGAYPGQAPPGAYPGAPGAYPGAPA
PGVYPGPPSGPGAYPSSGQPSAPGAYPATGPYGAPAGPLIVPYNLPLPGGVVPRMLITILGTVKP
NANRIALDFQRGNDVAFHFNPRFNENNRRVIVCNTKLDNNWGREERQSVFPFESGKPFKIQVLV
EPDHFKVAVNDAHLLQYNHRVKKLNEISKLGISGDIDLTSASYNMILEHHHHHH

Tetramer (coiled-coil: 'GCN4-pLI) amino acid sequence:
MASKGEELFTGVVPILVELDGDVNGHKFSVRGEGEGDATIGKLTLKFICTTGKLPVPWPTLVTTLT
YGVQCFSRYPDHMKRHDFFKSAMPEGYVQERTISFKDDGKYKTRAVVKFEGDTLVNRIELKGTD
FKEDGNILGHKLEYNFNSHNVYITADKQKNGIKANFTVRHNVEDGSVQLADHYQQNTPIGDGPVL
LPDNHYLSTQTVLSKDPNEKRDHMVLHEYVNAAGITLGMDELYKGGGSGGGSGGGSGGGSMARM
KQIEDKLEEILSKLYHIENELARIKKLLGEREFGGGSGGSGGGGSGGSGADNFSLHDALSGSGNP
NPQGWPGAWGNQPAGAGGYPGASYPGAYPGQAPPGAYPGQAPPGAYPGAPGAYPGAPAPG
VYPGPPSGPGAYPSSGQPSAPGAYPATGPYGAPAGPLIVPYNLPLPGGVVPRMLITILGTVKPNA

NRIALDFQRGNDVAFHFNPRFNENNRRVIVCNTKLDNNWGREERQSVFPFESGKPFKIQVLVEP
DHFKVAVNDAHLLQYNHRVKKLNEISKLGISGDIDLTSASYNMILEHHHHHH

Pentamer (coiled-coil: 'CC-Pent') amino acid sequence:
MASKGEELFTGVVPILVELDGDVNGHKFSVRGEGEGDATIGKLTLKFICTTGKLPVPWPTLVTTLT
YGVQCFSRYPDHMKRHDFFKSAMPEGYVQERTISFKDDGKYKTRAVVKFEGDTLVNRIELKGTD
FKEDGNILGHKLEYNFNSHNVYITADKQKNGIKANFTVRHNVEDGSVQLADHYQQNTPIGDGPVL
LPDNHYLSTQTVLSKDPNEKRDHMVLHEYVNAAGITLGMDELYKGGGSGGSGGSGGGSGKIEQ
ILQKIEKILQKIEWILQKIEQILQGEFGGGSGGSGGGGSGGSGADNFSLHDALSGSGNPNPQGWP
GAWGNQPAGAGGYPGASYPGAYPGQAPPGAYPGQAPPGAYPGAPGAYPGAPAPGVYPGPPS
GPGAYPSSGQPSAPGAYPATGPYGAPAGPLIVPYNLPLPGGVVPRMLITILGTVKPNANRIALDF
QRGNDVAFHFNPRFNENNRRVIVCNTKLDNNWGREERQSVFPFESGKPFKIQVLVEPDHFKVA
VNDAHLLQYNHRVKKLNEISKLGISGDIDLTSASYNMILEHHHHHH

Hexamer (coiled-coil: 'CC-Hex') amino acid sequence:
MASKGEELFTGVVPILVELDGDVNGHKFSVRGEGEGDATIGKLTLKFICTTGKLPVPWPTLVTTLT
YGVQCFSRYPDHMKRHDFFKSAMPEGYVQERTISFKDDGKYKTRAVVKFEGDTLVNRIELKGTD
FKEDGNILGHKLEYNFNSHNVYITADKQKNGIKANFTVRHNVEDGSVQLADHYQQNTPIGDGPVL
LPDNHYLSTQTVLSKDPNEKRDHMVLHEYVNAAGITLGMDELYKGGGSGGSGGSGGGSGGELKA
IAQELKAIAKELKAIAWELKAIAQGAGEFGGGSGGSGGGGSGGSGADNFSLHDALSGSGNPNPQ
GWPGAWGNQPAGAGGYPGASYPGAYPGQAPPGAYPGQAPPGAYPGAPGAYPGAPAPGVYP
GPPSGPGAYPSSGQPSAPGAYPATGPYGAPAGPLIVPYNLPLPGGVVPRMLITILGTVKPNANRI
ALDFQRGNDVAFHFNPRFNENNRRVIVCNTKLDNNWGREERQSVFPFESGKPFKIQVLVEPDHF
KVAVNDAHLLQYNHRVKKLNEISKLGISGDIDLTSASYNMILEHHHHHH